Theory of fully developed hydrodynamic turbulent flow: Applications of renormalization-group methods

Jian-Yang Yuan and David Ronis
Department of Chemistry, McGill University, 801 Sherbrooke Street, West Montreal, Quebec, Canada H3A 2K6
(Received 17 May 1991)

A model for randomly stirred or homogeneous turbulent fluids is analyzed using renormalization-group methods on a path-integral representation of the Navier-Stokes equations containing a spatially and temporally colored noise source. For moderate Reynolds numbers and certain values of the dynamic exponent governing the noise correlation, an additional scaling regime is found at wave vectors k beyond those where the Kolmogorov $\frac{5}{3}$ law holds. In this case, the energy spectrum decays as k^{-1-z}, where $1<z<2$, the fluid homodyne-scattering function decays as $(\text{time})^{-2/z}$, and the velocity-distribution function (as characterized by its skewness) deviates from a Gaussian. The additional scaling region disappears, and the Kolmogorov constant and Prandtl number become universal in the limit of infinite Reynolds number. In three spatial dimensions, the latter two equal $\frac{3}{2}(\frac{5}{3})^{1/3}$ and $\sqrt{0.8}$, respectively. The recent homodyne scattering experiments of Tong and co-workers [Phys. Rev. Lett. **65**, 2780 (1990)] are analyzed, and the connection of the new scaling region with intermittency is discussed.

PACS number(s): 47.25.−c, 05.40.+j, 42.25.Kb

I. INTRODUCTION

Self-similar features of homogeneous turbulence were first discussed by Richardson [1] and by Kolmogorov [2]. According to Kolmogorov's theory, in the cascade or scaling region, the turbulent part of the kinetic energy of the fluid is transferred, without dissipation, from larger length scales to smaller ones until the dissipative scale is reached. Hence, the normal kinematic viscosity plays no role in this scaling range, which is often referred to as the inertial range. As a consequence, dimensional analysis implies that the turbulent fluid's kinetic-energy spectrum $E(k)$ and the effective viscosity $\nu(k)$ must satisfy $E(k)=C_{\text{Kol}}\varepsilon_0^{2/3}k^{-5/3}$ and $\nu(k)\propto\varepsilon_0^{1/3}k^{-4/3}$, respectively, where k is the wave vector, and ε_0 is the energy injection rate per unit mass of fluid. Moreover, ε_0 is assumed to be absolutely constant in both time and space, and the Kolmogorov constant C_{Kol} is believed to be universal.

The assumption that ε_0 is absolutely constant requires that spatial and temporal fluctuations in ε_0 be ignored, i.e., the nonuniformities in energy transfer in the inertial range [3,4]. These fluctuations may result in intermittency that can manifest itself in several ways. For example, the energy spectrum may decay faster than the $\frac{5}{3}$ law and the velocity probability distribution can have large deviations from a Gaussian. The simplest measures of the deviation of the velocity distribution from a Gaussian are given by normalized cumulants such as the skewness,

$$s(r)\equiv\frac{\langle[v_r(\mathbf{r})-v_r(0)]^3\rangle}{\langle[v_r(\mathbf{r})-v_r(0)]^2\rangle^{3/2}}\ , \tag{1.1}$$

and the flatness,

$$\delta(r)\equiv\frac{\langle[v_r(\mathbf{r})-v_r(0)]^4\rangle}{\langle[v_r(\mathbf{r})-v_r(0)]^2\rangle^{2}}\ , \tag{1.2}$$

where $v_r(\mathbf{r})$ is the radial component of the fluid velocity field, $\mathbf{v}(\mathbf{r},t)$, and the angular brackets denote an average.

The skewness is a constant in the inertial range in the Kolmogorov theory. However, in an intermittently turbulent fluid, in the small-r limit, the skewness should diverge for small distances, thereby showing strong deviations from a Gaussian distribution. By postulating an asymptotic behavior of the variance of the logarithm of energy dissipation as $\sigma^2_{\ln\varepsilon}\sim A+9B\ln(L/l_d)$, where L is the scale where energy is injected, l_d is the scale where the viscous damping becomes important, and B is a positive number, Kolmogorov [4] showed that $E(k)\sim k^{-5/3-B}$ and that $s(r)\sim r^{-3B/2}$. Since then several models have been proposed to describe intermittency [5–9].

In most models, with the notable exception of Ref. [9], the Reynolds number R_e never plays an important role, in that corrections to the $\frac{5}{3}$ law are independent of R_e. In reality, however, experiments show nontrivial R_e dependence [10], although for sufficiently large Reynolds number, the Kolmogorov behavior of a turbulent fluid is observed at scales smaller than the energy injection scale L, while intermittency is observed at even smaller scales. These two regions are separated by a crossover scale l_c. As the Reynolds number is further increased the crossover scale l_c is reduced, ultimately approaching the dissipation scale l_d. As $R_e\to\infty$, the Kolmogorov $\frac{5}{3}$ law should be observed at all relevant scales. This scenario is depicted in Fig. 1.

The preceding discussion implies that the Reynolds number plays a crucial role in the inertial range, small-scale intermittency regions and dissipative ranges, and moreover, that the Kolmogorov region is a universal limit of turbulent fluids as $R_e\to\infty$. Thus, the energy spectrum should also be a function of Reynolds number, having the form

$$E(k)=\psi(kl_c(R_e))\varepsilon_0^{2/3}k^{-5/3}\ , \tag{1.3}$$

where $l_c(R_e)$ is the crossover length. Whether either $\psi(x)$ or $l_c(R_e)$ is universal is not obvious; nonetheless, we expect that

$$\lim_{R_e\to\infty} l_c(R_e)=l_d \tag{1.3a}$$

and that

$$\psi(x)\sim\begin{cases}C_{\rm Kol} & \text{as } x\to 0\\ x^{-(\eta-5/3)} & \text{for } 1\ll x\ll l_c(R_e)/l_d\ .\end{cases} \tag{1.3b}$$

With this type of crossover function, the energy spectrum in the intermittency region becomes $E(k)\sim k^{-\eta}$, where we expect that $\eta>\frac{5}{3}$.

The application of renormalization-group methods to the study of the dynamical properties of systems with an infinite number of degrees of freedom has resulted in powerful tools for studying scaling properties and calculating exponents or crossover functions [11–13]. The scaling and universal aspects of isotropic turbulent fluids suggest that renormalization-group methods can be used to advantage here as well [14–17]. The starting point in such calculations is the nonlinear Navier-Stokes equations to which a stochastic force, or noise, with certain assumed statistical properties, is added.

Recently, Yakhot and co-workers [16] generalized the work of Forster, Nelson, and Stephen [14] on fluids with a random stirring force, and applied their results to model a turbulent fluid. For a given wave vector k and frequency ω, the random stirring force correlation functions $\Omega(k,\omega)$ used in Refs. [14] and [16] can be written in the form

$$\Omega(k,\omega)=2\chi k^{-y}\ , \tag{1.4}$$

with implied upper and lower cutoffs in k, i.e., l_d^{-1} and L^{-1}, respectively (cf. Fig. 1). The exponent y is set to -2 or 0 in models A or B of Ref. [14], respectively. In Ref. [16], the choice $y=d$ was made in order to obtain Kolmogorov's $\frac{5}{3}$ law in the small-wave-vector (ir) limit.

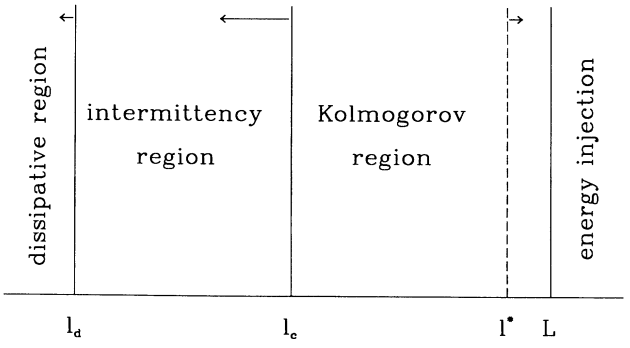

FIG. 1. Characteristic regions in turbulent flows and their crossover length scales. $l^*\equiv 1/\kappa^*$, cf. Eq. (3.47). The arrows indicate the directions in which the crossover scales move when the Reynolds number is increased (cf. Sec. III). Note that the intermittency crossover scale is a strong function of the Reynolds number, cf. Eq. (3.49), and will merge with the dissipative scale.

As was noted by Ronis [17] the analysis of Ref. [16] ignores the renormalization of the noise-correlation amplitude, and by including it, Ronis [17] was able to obtain Kolmogorov's $\frac{5}{3}$ law in either the ir or uv (large-wave-vector) limits depending on the choice of exponents.

One obvious objection to these approaches is that they completely ignore the actual generation of the turbulence, e.g., at the boundaries of the system, and the precise nature of the stirring force is not clear. Indeed, there is no *a priori* theory of the exponents used to characterize the random-force autocorrelation function in applications to nonequilibrium fluids (this is not the case near equilibrium, where the Einstein-Nyquist relations [18] can be used [19]).

In order to shed some light on this last point, consider the Navier-Stokes equations for an incompressible fluid with density ρ, kinematic viscosity ν, and hydrostatic pressure p_h; i.e.,

$$\frac{\partial\mathbf{v}(\mathbf{r},t)}{\partial t}+\mathbf{v}(\mathbf{r},t)\cdot\nabla\mathbf{v}(\mathbf{r},t)=-\nabla\left[\frac{p_h(\mathbf{r},t)}{\rho}\right]+\nu\nabla^2\mathbf{v}(\mathbf{r},t)+\mathbf{F}(\mathbf{r},t)\ , \tag{1.5}$$

where incompressibility implies that

$$\nabla\cdot\mathbf{v}(\mathbf{r},t)=0\ . \tag{1.6}$$

The force $\mathbf{F}(\mathbf{r},t)$ results from the interactions with the boundaries, and as such is not stochastic in nature. Hence, how does a statistical force arise?

Two possibilities suggest themselves. First, the instability of the fluid motion may lead to a large amplification of the random forces associated with thermal fluctuations [20], as was recently demonstrated for the Lorenz equations [21]. It is not obvious that this is the case here, and moreover, if it is, then key elements of the Kolmogorov picture must be abandoned. A second possibility is that the random force represents an effective force felt at smaller length scales that results from the turbulent, but deterministic, motion at larger scales (i.e., at scales $\gtrsim L$) as transmitted by the nonlinear terms in the Navier-Stokes equations. Of course, this only happens outside the dissipative range, where such influences quickly decay before they can affect the fluid motion. In most works on turbulent fluids, it is the second possibility that is considered to be more likely, and we adopt the same viewpoint here.

The convective terms in the Navier-Stokes equations, in addition to transferring energy from the injection scale into the cascade, also transmit other aspects of the long-wavelength fluid motions which can affect the small scale motions. For example, a vortex can be deformed by a larger scale motion, thereby modifying its internal motion, and the details of the resulting motion will depend on more than just the energy injected into the cascade.

In order to examine the second possibility more carefully, we introduce a projection operator $\mathcal{P}$ such that

$$\mathbf{v}'(\mathbf{r},t)\equiv\mathcal{P}\mathbf{v}(\mathbf{r},t) \tag{1.7}$$

contains only short-wavelength information (in compar-

ison with the energy-injection scales). By applying $\mathcal{P}$ to the Navier-Stokes equations it follows that

$$\frac{\partial \mathbf{v}'(\mathbf{r},t)}{\partial t}+\mathbf{v}'(\mathbf{r},t)\cdot\nabla\mathbf{v}'(\mathbf{r},t)=-\frac{1}{\rho}\nabla p_h'(\mathbf{r},t)+\nu\nabla^2\mathbf{v}'(\mathbf{r},t)+\mathbf{f}(\mathbf{r},t)\ , \tag{1.8}$$

where

$$\mathbf{f}(\mathbf{r},t)\equiv\mathcal{P}\mathbf{F}(\mathbf{r},t)-\mathcal{P}[\mathbf{v}(\mathbf{r},t)\cdot\nabla\mathbf{v}(\mathbf{r},t)]+\mathbf{v}'(\mathbf{r},t)\cdot\nabla\mathbf{v}'(\mathbf{r},t)\ . \tag{1.9}$$

This new force contains information about boundaries as well as the mode-coupling effects associated with velocity components on the injection scale. Away from boundaries, we expect that $\mathcal{P}\mathbf{F}(\mathbf{r},t)=0$, and hence, the random stirring force used in renormalization-group studies in essence results from the mode coupling between the motion on the L scale with that on the smaller ones. Since the motion on all scales is expected to be chaotic, including that on the L scale, we expect that $\mathbf{f}(\mathbf{r},t)$ will have complicated, chaotic time and space dependences, and it is this quantity which is actually modeled by a stochastic force in random stirring models of turbulence.

In this work, we assume that the transverse parts of $\mathbf{f}(\mathbf{r},t)$ have Gaussian statistics, and write the autocorrelation function as [22,23]

$$\langle \mathbf{f}(\mathbf{k},\omega)\mathbf{f}(\mathbf{k}',\omega')\rangle=(2\pi)^{d+1}\delta(\mathbf{k}+\mathbf{k}')\times\delta(\omega+\omega')(\overleftrightarrow{\mathbf{1}}-\hat{\mathbf{k}}\hat{\mathbf{k}})\Omega(k,\omega). \tag{1.10}$$

(Henceforth, the prime on the projected velocity field will be omitted.) In the theories presented in Refs. [15–17], only a single exponent for the energy spectrum is obtained in the nontrivial-scaling regions; intermittency or crossover phenomena are not found. Apparently something is missing, and within the framework of these approaches, the only place to look for the answer is in the assumed form of the noise-correlation function.

A key feature of the earlier renormalization-group studies on turbulence is the assumption of a zero noise-correlation time (i.e., white noise), although at the same time a nontrivial spatial correlation is introduced. The assumption of white noise is at best a reasonable approximation to the true correlations of $\mathbf{f}(\mathbf{r},t)$, and in fact, there seems no objective reason, except for technical simplicity, why this has to be so. Indeed, by imaging turbulent fluids near boundaries, e.g., in grid flows [24], it becomes clear that fluid motion has strong temporal and spatial correlations. Since $\mathbf{f}(\mathbf{r},t)$ models the effects of the boundaries and large-scale motions on the smaller ones, it seems quite unlikely that the random force is uncorrelated in time while having strong spatially correlations (e.g., the random force correlation remains constant as $r\to\infty$ for $y=d$).

One objection to a nonzero correlation time is that the resulting theory would not be invariant under Galilean transformation: $\mathbf{k}'=\mathbf{k}$, $\omega'=\omega+\mathbf{k}\cdot\mathbf{u}$, where $\mathbf{u}$ is the Galilean velocity shift. However, since the random forces represent the effects of boundaries, and these are not included in the Galilean transformation, there is no *a priori* reason why global Galilean invariance must hold. Nonetheless, it is commonly believed that the scaling phenomena of turbulent flows are Galilean invariant. This imposes constraints on the form of the noise correlations. For example, let $\tau(k)$ be the characteristic decay time of the $\mathbf{f}(\mathbf{k},t)$ correlations. The theory will be approximately Galilean invariant if $uk\tau(k)\ll 1$ for $kL>1$.

This paper is organized as follows: In the following section, we set up the theory, which is subsequently renormalized in Sec. III. By identifying the exponents governing the Kolmogorov part of the energy spectrum, we determine some of the parameters appearing in the model. Different forms for the noise are analyzed and discussed. Significantly, if the correlation time of the noise is sufficiently long [i.e., compared to the bare-shear relaxation time $(\nu k^2)^{-1}$] and the Reynolds number is not too high, then a crossover to a new scaling regime can be observed in the kinetic-energy spectrum. In Sec. IV we study the skewness of the two-point velocity-distribution function and find large deviations from Kolmogorov scaling in this crossover region; we also discuss the diffusion of a passive scalar and compare with some recent experimental results. Finally, Sec. V contains a summary and some concluding remarks.

II. DEFINITIONS AND PRELIMINARY REMARKS

As was discussed in the Introduction, we will model the effects of the turbulent motion on the L scale by an effective noise-correlation function that reflects both the temporal and spatial coherences in the forcing of turbulent fluids, even if at the phenomenological level. With this in mind, we modify the commonly used noise correlation $\Omega(k,\omega)$ and assume that

$$\Omega(k,\omega)\equiv\frac{2\chi\mu^2k^{-y+2z}}{\omega^2+\mu^2k^{2z}}\ , \tag{2.1}$$

where $\mu>0$. The exponent y is as yet undetermined. Approximate Galilean invariance, as discussed in the Introduction, requires that $z>1$, but imposes no other constraint. (As it turns out, below, integrability of the renormalized energy spectrum also requires that $z>1$ when $d=3$.)

The corresponding random force time correlations decay as $\exp(-\mu k^z t)$, and the equal-time random force correlation function decays as r^{y-z-d} as $r\to\infty$. The model reduces to the white-noise model discussed in Ref. [17] when $\mu\to\infty$ or $z\to+\infty$,

As was done in Ref. [17], we will analyze this problem by using the field-theoretical-renormalization-group method. The calculation is based on the Martin-Siggia-Rose [11] (MSR) path-integral representation of the moment-generating functional Ξ obtained from the fluctuating Navier-Stokes equations, cf. Eqs. (1.6) and (1.8). By averaging over the noise $\mathbf{f}$, and using Eq. (1.10), the moment generating functional becomes

$$\Xi[\xi(\mathbf{r},t),\zeta(\mathbf{r},t)]=\int\mathcal{D}[\mathbf{v}(\mathbf{r},t)]\mathcal{D}[\bar{\mathbf{v}}(\mathbf{r},t)]\,e^{i\mathcal{L}}\ , \tag{2.2}$$

where the Lagrangian

$$\mathcal{L}\equiv\frac{1}{(2\pi)^{d+1}}\int d\mathbf{k}\,d\omega\left[(i\omega+\nu k^2)\tilde{\mathbf{v}}(-\mathbf{k},-\omega)\cdot\mathbf{v}(\mathbf{k},\omega)+\frac{i}{2}\Omega(k,\omega)\tilde{\mathbf{v}}(-\mathbf{k},-\omega)\cdot\overleftrightarrow{\Phi}_{\mathbf{k}}\cdot\tilde{\mathbf{v}}(\mathbf{k},\omega)\right.$$
$$+\boldsymbol{\xi}(-\mathbf{k},-\omega)\cdot\mathbf{v}(\mathbf{k},\omega)+\boldsymbol{\zeta}(-\mathbf{k},-\omega)\cdot\tilde{\mathbf{v}}(\mathbf{k},\omega)$$
$$\left.-\frac{i\lambda}{2}\frac{1}{(2\pi)^{d+1}}\int d\mathbf{k}_1 d\omega_1\tilde{v}^{\alpha}(-\mathbf{k},-\omega)V_{\mathbf{k}}^{\alpha;\beta,\gamma}v^{\beta}(\mathbf{k}-\mathbf{k}_1,\omega-\omega_1)v^{\gamma}(\mathbf{k}_1,\omega_1)\right], \tag{2.3}$$

$\boldsymbol{\xi}(\mathbf{k},\omega)$ and $\boldsymbol{\zeta}(\mathbf{k},\omega)$ are currents conjugate to $\mathbf{v}(\mathbf{k},\omega)$ and its adjoint field $\tilde{\mathbf{v}}(\mathbf{k},\omega)$, respectively, $\overleftrightarrow{\Phi}_{\mathbf{k}}\equiv\overleftrightarrow{\mathbf{1}}-\hat{\mathbf{k}}\hat{\mathbf{k}}$, and

$$V_{\mathbf{k}}^{\alpha;\beta,\gamma}\equiv k^{\beta}\Phi_{\mathbf{k}}^{\alpha,\gamma}+k^{\gamma}\Phi_{\mathbf{k}}^{\alpha,\beta}\,. \tag{2.4}$$

The greek superscripts denote Cartesian coordinates, and sums over repeated indices are implied hereafter. The parameter λ is introduced for the purpose of ordering a naive perturbation expansion and it will ultimately be set to unity. Remember that the fluid is assumed to be incompressible, and hence, the domains of the path integration are restricted to those fields where $\mathbf{k}\cdot\mathbf{v}=0$.

It is easy to see that all moments of the velocity distribution are obtained by functional differentiation of $\ln\Xi$. For example, the average fields $\langle\mathbf{v}\rangle$ and $\langle\tilde{\mathbf{v}}\rangle$ are given by

$$\langle\mathbf{v}(\mathbf{k},\omega)\rangle=\left.\frac{\delta\ln\Xi(\xi,\zeta)}{\delta\xi(-\mathbf{k},-\omega)}\right|_{\xi=\zeta=0} \tag{2.5a}$$

and

$$\langle\tilde{\mathbf{v}}(\mathbf{k},\omega)\rangle=\left.\frac{\delta\ln\Xi(\xi,\zeta)}{\delta\zeta(-\mathbf{k},-\omega)}\right|_{\xi=\zeta=0}. \tag{2.5b}$$

By treating the quadratic terms in $\mathcal{L}$ as the free part of the Lagrangian, we can formally generate a perturbation expansion in the convective terms contained in $V_{\mathbf{k}}^{\alpha;\beta,\gamma}$; i.e., in λ. For $\boldsymbol{\xi}(\mathbf{r},t)=\boldsymbol{\zeta}(\mathbf{r},t)=0$, it follows that corresponding zeroth-order averages, denoted by $\langle\ \rangle_0$, become

$$\langle v^{\alpha}(\mathbf{k},\omega)v^{\beta}(\mathbf{k}',\omega')\rangle_0=\frac{\Omega(k,\omega)}{\omega^2+\nu^2k^4}\Phi_{\mathbf{k}}^{\alpha,\beta}(2\pi)^{d+1}\delta(\mathbf{k}+\mathbf{k}')\delta(\omega+\omega')\equiv\ \text{———————}\ , \tag{2.6a}$$

$$\langle\tilde{v}^{\alpha}(\mathbf{k},\omega)v^{\beta}(\mathbf{k}',\omega')\rangle_0=\frac{i}{-i\omega+\nu k^2}\Phi_{\mathbf{k}}^{\alpha,\beta}(2\pi)^{d+1}\delta(\mathbf{k}+\mathbf{k}')\delta(\omega+\omega')\equiv\ \text{WWWWWW———}\ , \tag{2.6b}$$

$$\langle v^{\alpha}(\mathbf{k},\omega)\tilde{v}^{\beta}(\mathbf{k}',\omega')\rangle_0=\frac{i}{i\omega+\nu k^2}\Phi_{\mathbf{k}}^{\alpha,\beta}(2\pi)^{d+1}\delta(\mathbf{k}+\mathbf{k}')\delta(\omega+\omega')\equiv\ \text{———WWWWWW}\ , \tag{2.6c}$$

and

$$\langle\tilde{v}^{\alpha}(\mathbf{k},\omega)\tilde{v}^{\beta}(\mathbf{k}',\omega')\rangle_0=0\,. \tag{2.6d}$$

All zeroth-order correlation functions containing an odd number of fields vanish and the rest can be expressed in terms of the two-field correlation functions, cf. Eqs. (2.6a)–(2.6d), by summing over all possible ways of factorization.

As is well known, this kind of perturbation theory fails for turbulent fluids. Furthermore, the difficulties with the naive perturbation theory are similar to those encountered in the study of field theories for systems with an infinite number of degrees of freedom. The ultimate goal of the renormalization-group methods is to deal with the divergences in the naive perturbation theories in the strong-interaction limit. The starting point in the renormalization-group analysis is the loop expansion [25] of a new generating functional Γ defined as

$$\Gamma[\langle\mathbf{v}(\mathbf{r},t)\rangle,\langle\tilde{\mathbf{v}}(\mathbf{r},t)\rangle]\equiv-\ln\Xi+\frac{1}{(2\pi)^{d+1}}\int d\mathbf{k}\,d\omega[\boldsymbol{\xi}(-\mathbf{k},-\omega)\cdot\langle\mathbf{v}(\mathbf{k},\omega)\rangle+\boldsymbol{\zeta}(-\mathbf{k},-\omega)\cdot\langle\tilde{\mathbf{v}}(\mathbf{k},\omega)\rangle]\,. \tag{2.7}$$

This new generating functional is the generator of the equations of motion and one-particle-irreducible (1PI) vertex functions, from which all the correlation functions can be computed. For example,

$$\left.\frac{\delta\Gamma[\langle\mathbf{v}\rangle,\langle\tilde{\mathbf{v}}\rangle]}{\delta\langle\tilde{\mathbf{v}}(\mathbf{r},t)\rangle}\right|_{\langle\tilde{\mathbf{v}}(\mathbf{r},t)\rangle=0}=0 \tag{2.8}$$

generates an equation of motion for the average velocity.

In addition, the new generating functional and the loop expansion reorders terms such that the terms with same degree of divergence can be directly treated together [26].

The one-loop corrections to the viscosity, the noise correlation, and the nonlinear coupling constant can be easily obtained. Their diagrammatic representations are shown in Fig. 2. If the uv cutoff is taken to infinity, the integrals corresponding to the diagrams shown in Fig. 2 diverge for certain values of the parameters. In particu-

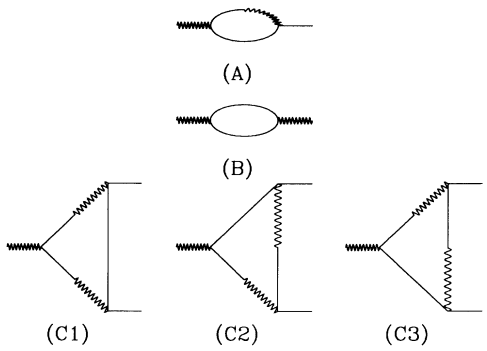

FIG. 2. Diagrammatic representation of the one-loop corrections to the primitively divergent vertex functions. The propagator and correlation function lines are defined in the text, cf. Eq. (2.6).

lar, simple power-counting arguments show that the correction to the viscosity is marginal in the uv (i.e., diverges logarithmically) when

$$\varepsilon \equiv \begin{cases} 4+y-d \text{ for } z \geq 2 \\ 6+y-d-z \text{ for } z<2 \end{cases} \tag{2.9}$$

vanishes. Similarly, the correction to the noise correlation function becomes marginal when

$$\varepsilon' \equiv \varepsilon+2+y \tag{2.10}$$

vanishes. These divergences are obviously primitive [26].

The integrals may also diverge in the ir when the external wave vectors and frequencies are set to zero. Convergence in the ir, with concomitant super-renormalizability, is guaranteed for negative ε_{ir} and $\varepsilon'_{ir} \equiv \varepsilon_{ir}+2+y$, where

$$\varepsilon_{ir} \equiv \begin{cases} 4+y-d \text{ for } z<2 \\ 6+y-d-z \text{ for } z \geq 2 \ . \end{cases} \tag{2.11}$$

It is easy to see that the uv marginal diagrams are always convergent in the ir for $z \neq 2$ (they become ir marginal for $z=2$ or white noise). Note that it is possible to choose exponents such that both ε and ε' are positive with both ε_{ir} and ε'_{ir} negative, thereby making the diagrams simultaneously convergent in both the ir and uv. Moreover, it is readily shown that the theory is renormalizable in the sense that only a finite number of counterterms or renormalization parameters are needed to eliminate the divergences in the theory [26].

When $z>2$, the preceding observations about the uv behavior are identical to those made in Ref. [17]. This should not be surprising, since the case $z>2$ corresponds to noise whose correlation time is shorter (in the uv limit) than the time scale of normal shear fluctuations, and hence, it becomes equivalent to white noise. On the other hand, when $z<2$ the reverse is true, and, as we will show below, this leads to some interesting differences from the white-noise case.

The first step in developing a renormalization scheme is to absorb the primitive divergences by introducing renormalized parameters and corresponding counterterms in the Lagrangian. This requires that all divergences be simultaneously marginal, and hence, the perturbation theory must be performed around $\varepsilon=\varepsilon'=0$. Specifically, this requires that an the expansion be performed around $y=-2$ and the critical dimension

$$d_c = \begin{cases} 4-z \text{ for } z<2 \\ 2 \text{ for } z \geq 2 \ . \end{cases}$$

Incidentally, $y=-2$ is just what the Einstein-Nyquist relations would imply [18,19].

We now turn to the details of the perturbative expansion and of the renormalization.

III. RENORMALIZATION AND DETAILED ANALYSIS

The terms in the naive perturbation expansion contain logarithmic divergences when ε and ε' vanish. These signal the existence of badly converging perturbation expansions. Nonetheless, in a renormalizable theory, the number of such divergences is finite, and moreover, *even though the associated perturbation expansions cannot be explicitly summed*, are assumed to sum to some finite answer (e.g., the renormalized viscosity). Note that the renormalized parameters are not equal to the corresponding bare parameters; here, all we can say is that they are proportional. In addition, they are not the same as the effective wave-vector or frequency-dependent parameters often introduced in turbulence theories (and often referred to as renormalized viscosity). Here, the renormalized parameters are independent of frequency and wave vector.

There is still some freedom in choosing what to formally resum into the renormalized parameters. For technical simplicity, we follow the minimal subtraction scheme [27], and subtract poles in ε or ε' in the loop corrections to primitively divergent vertex functions by multiplicatively or additively redefining the relevant parameters in the model. When the singular parts (in ε or ε') of the diagrams shown in Fig. 2 are computed, it turns out that no additive renormalizations are needed at one-loop order. The multiplicative renormalization conditions are found by solving the following equations:

$$i\nu k^2 \Phi^{\alpha,\beta}_{\mathbf{k}} + \lambda^2 K^{\alpha,\beta}_{\nu}(\mathbf{k},\omega) = i\nu_R k^2 \Phi^{\alpha,\beta}_{\mathbf{k}} \ , \tag{3.1}$$

$$\Omega(k,\omega)\Phi^{\alpha,\beta}_{\mathbf{k}} - \frac{\lambda^2}{2} K^{\alpha,\beta}_{\Omega}(\mathbf{k},\omega) = \Omega_R(k,\omega)\Phi^{\alpha,\beta}_{\mathbf{k}} \ , \tag{3.2}$$

and

$$\lambda V^{\alpha;\beta,\gamma}_{\mathbf{k}} + 3\lambda^3 K^{\alpha;\beta,\gamma}_{\lambda}(\mathbf{k},\omega;\mathbf{k}_1,\omega_1) = \lambda_R V^{\alpha;\beta,\gamma}_{\mathbf{k}} \ , \tag{3.3}$$

where, to the one-loop order,

$$K^{\alpha,\beta}_{\nu} \equiv \frac{2i\chi\mu^2}{(2\pi)^{d+1}} \int d\mathbf{k}_1 d\omega_1 \frac{V^{\alpha;\gamma_1,\gamma}_{\mathbf{k}} V^{\gamma_1;\beta_1,\beta}_{\mathbf{k}-\mathbf{k}_1} \Phi^{\gamma,\beta_1}_{\mathbf{k}_1} k_1^{-y+2z}}{(\omega_1^2+\mu^2 k_1^{2z})(\omega_1^2+\nu^2 k_1^4)[i(\omega-\omega_1)+\nu|\mathbf{k}-\mathbf{k}_1|^2]} \ , \tag{3.4}$$

$$K_{\Omega}^{\alpha,\beta} \equiv \frac{4\chi^2\mu^4 V_{-\mathbf{k}}^{\alpha;\gamma,\gamma_1} V_{\mathbf{k}}^{\beta;\alpha_1,\beta_1}}{(2\pi)^{d+1}} \int d\mathbf{k}_1 d\omega_1 \frac{\Phi_{\mathbf{k}-\mathbf{k}_1}^{\gamma,\alpha_1} \Phi_{\mathbf{k}_1}^{\gamma_1,\beta_1} k_1^{-y+2z} |\mathbf{k}-\mathbf{k}_1|^{-y+2z}}{(\omega_1^2+\mu^2 k_1^{2z})(\omega_1^2+\nu^2 k_1^4)[(\omega-\omega_1)^2+\mu^2|\mathbf{k}-\mathbf{k}_1|^{2z}][(\omega-\omega_1)^2+\nu^2|\mathbf{k}-\mathbf{k}_1|^4]} , \tag{3.5}$$

and

$$K_{\lambda}^{\alpha;\beta,\gamma} \equiv -\frac{2\chi\mu^2 V_{\mathbf{k}}^{\alpha;\beta_1,\beta_2}}{(2\pi)^{d+1}} \int d\mathbf{k}_2 d\omega_2 \frac{V_{\mathbf{k}-\mathbf{k}_1+\mathbf{k}_2}^{\beta_1;\beta,\gamma_1} \Phi_{\mathbf{k}_2}^{\gamma_1,\gamma_2} k_2^{-y+2z}}{(\omega_2^2+\mu^2 k_2^{2z})(\omega_2^2+\nu^2 k_2^4)[i(\omega-\omega_1+\omega_2)+\nu|\mathbf{k}-\mathbf{k}_1+\mathbf{k}_2|^2]}$$
$$\times \left[\frac{V_{\mathbf{k}_1-\mathbf{k}_2}^{\beta_2;\gamma,\gamma_2}}{i(\omega_1-\omega_2)+\nu|\mathbf{k}_1-\mathbf{k}_2|^2} + \frac{2V_{\mathbf{k}+\mathbf{k}_2}^{\beta_2;\beta_1,\gamma}}{i(\omega+\omega_2)+\nu|\mathbf{k}+\mathbf{k}_2|^2} \right] . \tag{3.6}$$

As was mentioned above, some of the integrals given by the preceding expressions diverge logarithmically when the uv cutoff is taken to infinity, and ε and ε' set to zero. In the minimal-subtraction method, the cutoff is assumed infinite, and integrals are evaluated just below the critical dimension. The singularities in ε and ε' are then eliminated by multiplicatively renormalizing the bare parameters in the model (e.g., ν, χ, etc.). The same approach is followed here, with the additional assumption that $\varepsilon/\varepsilon'=O(1)$ [17]. In addition, we shall evaluate the integrals at the external momentum $k=\kappa$ and zero external frequency [28]. We thus find that

$$\nu=\nu_R \left[1-\frac{g(z)}{\varepsilon} \right] , \tag{3.7}$$

where

$$g(z) \equiv \begin{cases} \sigma A_d u_R \text{ for } z \neq 2 \\ \dfrac{A_d u_R \mu_R (3\nu_R^2+2\mu_R\nu_R+\mu_R^2)}{(\nu_R+\mu_R)^3} \text{ for } z=2 , \end{cases} \tag{3.8}$$

with

$$A_d \equiv \frac{S_d(d^2-2)}{2d(d+2)(2\pi)^d} , \tag{3.9}$$

$$\sigma \equiv \begin{cases} \dfrac{2(d^2-d+2)}{(d^2-2)} \text{ for } z<2 \\ 1 \text{ for } z>2 , \end{cases} \tag{3.10}$$

$$S_d \equiv \frac{2\pi^{d/2}}{\Gamma(d/2)} \tag{3.11}$$

is the volume of a d-dimensional unit sphere, and

$$u_R \equiv \begin{cases} \dfrac{\lambda_R^2 \chi_R \kappa^{-\varepsilon}}{\nu_R^3} \text{ for } z \geq 2 \\ \dfrac{\lambda_R^2 \chi_R \mu_R \kappa^{-\varepsilon}}{\nu_R^4} \text{ for } z<2 \end{cases} \tag{3.12}$$

can be viewed as a dimensionless expansion parameter. Similarly,

$$\chi=\chi_R \left[1-\frac{f(z)}{\varepsilon'} \right] , \tag{3.13}$$

where

$$f(z) \equiv \begin{cases} A_d u_R \text{ for } z \neq 2 \\ \dfrac{A_d u_R \mu_R (\nu_R^2+3\mu_R\nu_R+\mu_R^2)}{(\nu_R+\mu_R)^3} \text{ for } z=2 . \end{cases} \tag{3.14}$$

Since the frequency corrections to $K_{\Omega}^{\alpha,\beta}$ are well behaved, no renormalization of μ is required to one-loop order. Finally, it is easy to show that the singularities in $K_{\lambda}^{\alpha;\beta,\gamma}$ all cancel (a consequence of the local Galilean invariance satisfied by the present model) and hence, $\lambda=\lambda_R$. Thus, we henceforth take $\lambda=1$ without any loss of generality.

Once the relationships between renormalized and bare quantities are established, we can easily derive renormalization-group equations. Since the bare theory is independent of the renormalization parameter κ, any quantity F in the bare theory must satisfy

$$\left[\frac{\partial F}{\partial \kappa} \right]_{\nu,\chi} = 0 . \tag{3.15}$$

By expressing F in terms of the renormalized parameters, Eq. (3.15) becomes

$$\kappa \left[\frac{\partial F}{\partial \kappa} \right]_{\nu_R,u_R} + \beta_u(u_R,\nu_R) \left[\frac{\partial F}{\partial u_R} \right]_{\nu_R,\kappa} + \beta_\nu(u_R,\nu_R) \left[\frac{\partial F}{\partial \nu_R} \right]_{u_R,\kappa} = 0 , \tag{3.16}$$

where

$$\beta_u(u_R,\nu_R) \equiv \kappa \left[\frac{\partial u_R}{\partial \kappa} \right]_{\nu,\chi} \tag{3.17}$$

and

$$\beta_\nu(u_R,\nu_R) \equiv \kappa \left[\frac{\partial \nu_R}{\partial \kappa} \right]_{\nu,\chi} \tag{3.18}$$

are the Wilson functions. By using Eqs. (3.7) and (3.13) in (3.17) and (3.18) and expanding the results to one-loop order, we find that

$$\beta_u(u_R,\nu_R)=\begin{cases}-\varepsilon u_R\left[1-\dfrac{u_R}{u^*}\right] & \text{for } z\neq 2\\ -\varepsilon u_R\left[1-\dfrac{A_d u_R\mu_R}{\varepsilon(\nu_R+\mu_R)^3}\left[3(3\nu_R^2+2\nu_R\mu_R+\mu_R^2)-(\nu_R^2+3\nu_R\mu_R+\mu_R^2)\dfrac{\varepsilon}{\varepsilon'}\right]\right] & \text{for } z=2\end{cases} \tag{3.19}$$

and

$$\beta_\nu(u_R,\nu_R)=\begin{cases}-A_d\sigma u_R\nu_R & \text{for } z\neq 2\\ -\dfrac{A_d u_R\nu_R\mu_R(3\nu_R^2+2\nu_R\mu_R+\mu_R^2)}{(\nu_R+\mu_R)^3} & \text{for } z=2\ ,\end{cases} \tag{3.20}$$

where

$$u^*\equiv\frac{\gamma}{A_d} \tag{3.21}$$

and

$$\gamma\equiv\begin{cases}\dfrac{\varepsilon}{3-\varepsilon/\varepsilon'} & \text{for } z\geq 2\\ \dfrac{\varepsilon}{4\sigma-\varepsilon/\varepsilon'} & \text{for } z<2\ .\end{cases} \tag{3.22}$$

The general form of the solutions to the renormalization-group equations may be determined using the method of characteristics [29]. The equations determining the invariants along the characteristics associated with Eq. (3.16) are

$$\kappa\frac{dU}{d\kappa}=-\beta_u(U,W) \tag{3.23}$$

and

$$\kappa\frac{dW}{d\kappa}=-\beta_\nu(U,W), \tag{3.24}$$

where, without loss of generality, we may assume that $U(1)=u_R$ and $W(1)=\nu_R$. These equations govern the flows in the parameter space and are differential forms of the recursion relations, cf. Eqs. (3.7) and (3.13). Moreover, as will become clear below, the renormalization-group equation imposes strong constraints on the allowed functional forms of physical quantities.

The fixed points of the renormalization-group transformation are found by solving

$$\beta_u(U,W)=0 \tag{3.25}$$

and

$$\beta_\nu(U,W)=0\ . \tag{3.26}$$

Two fixed-point solutions are found: (I) $U=0$ with W arbitrary; and (II) $U=u^*$ with $W=0$. The fixed point (I) is trivial and unimportant. In fact, as long as ν_R is finite we must immediately conclude that χ_R vanishes at this fixed point; hence, the random force vanishes. Similarly, if χ_R is finite, ν_R must be infinite (and the Reynolds number vanishes). We therefore conclude that this fixed point has little to do with a turbulent fluid. In contrast, the second fixed point leads to a vanishing effective viscosity, therefore, it is the strong interaction limit and we will focus our discussion on it.

When $z\neq 2$, it is easily shown [17] that the solutions to the characteristic equations are

$$U(\kappa)\equiv\frac{u_R u^*}{u_R+\kappa^{-\varepsilon}(u^*-u_R)} \tag{3.27}$$

and

$$W(\kappa)\equiv\nu_R\left[\frac{u^*\kappa^{-\varepsilon}}{u_R+\kappa^{-\varepsilon}(u^*-u_R)}\right]^{-\sigma\gamma/\varepsilon}. \tag{3.28}$$

With these last two expressions, it follows that the general solution to Eq. (3.16) for a quantity F with dimensionality $L^l T^\tau$ has form

$$F=R^{l}[W(\kappa R)R^{-2}]^{-\tau}\times G\left[\left\{R\mathbf{k}_i,\frac{\omega_i R^2}{W(\kappa R)}\right\}_{i=1}^{n},\frac{\mu_R R^{2-z}}{W(\kappa R)},U(\kappa R)\right], \tag{3.29}$$

where n is the number of external wave vectors and frequencies, R is an arbitrary length, and G is a dimensionless function, consistent with isotropic symmetry, but is otherwise undetermined (insofar as the renormalization-group equation is concerned).

The choice of R, the so-called match condition [30], is arbitrary, and may be used to analyze the scaling properties of the theory. For example, the simple match condition $Rk=1$ allows a two-point function to be rewritten as

$$F=k^{-l}[W(\kappa/k)k^2]^{-\tau}\times G\left[\frac{\omega}{W(\kappa/k)k^2},\frac{\mu_R k^{z-2}}{W(\kappa/k)},U(\kappa/k)\right], \tag{3.30}$$

cf. Eq. (3.29). The match-condition also allows us to connect the strongly interacting region of parameters with one where perturbation theory is applicable [30]. For example, since $U(\kappa/k)\to u^*\sim O(\varepsilon)$ as $k^\varepsilon\to 0$ and $U(\kappa/k)\to 0$ as $k^\varepsilon\to\infty$ the initial value curve for the method of characteristics may be chosen where perturbative expansions of the quantities of interest are valid (e.g., where $U\to 0$). The characteristic equations, via $U(\kappa/k)$ and $W(\kappa/k)$, map the perturbative expansions into the strongly interacting region.

In order to carry out this procedure, the renormalized parameters must be reexpressed in terms of the solutions to the characteristic equations; specifically, Eqs. (3.27) and (3.28) imply that

$$u_R = U(\kappa R)\left[1-\varepsilon\left[1-\frac{U(\kappa R)}{u^*}\right]\ln(\kappa R)+O(\varepsilon^2)\right] \tag{3.31}$$

and

$$\nu_R = W(\kappa R)\left[1-\sigma\gamma\frac{U(\kappa R)}{u^*}\ln(\kappa R)+O(\varepsilon^2)\right] . \tag{3.32}$$

In addition, since $(\kappa R)^{\varepsilon}=1+\varepsilon\ln(\kappa R)+O(\varepsilon^2)$, we have

$$\chi_R = \frac{R^{-\varepsilon}U(\kappa R)W^3(\kappa R)}{\mu_R}\left[1-\frac{\varepsilon\gamma U(\kappa R)}{\varepsilon' u^*}\ln(\kappa R)+O(\varepsilon^2)\right] \times \begin{cases} W(\kappa R) \text{ for } z<2 \\ \mu_R \text{ for } z>2 , \end{cases} \tag{3.33}$$

cf. Eq. (3.12). When these expressions are used in the renormalized loop expansion of a physical quantity, an expression valid in the strongly interacting limit is obtained (assuming the validity of the nonperturbative solutions of the renormalization-group equation). Moreover, explicit terms in $\ln(\kappa R)$ are inconsistent with Eq. (3.29) and must cancel to the appropriate order in the loop expansion, thereby providing a check on the perturbation theory.

As an example, consider the energy spectrum; in leading order in perturbation theory,

$$E(k)=\frac{S_d(d-1)\chi\mu k^{1-(6+y-z-d)}}{2(2\pi)^d\nu(\nu+\mu k^{z-2})}+O(\varepsilon) , \tag{3.34}$$

which, upon carrying out the steps described above, becomes

$$E(k)=\frac{S_d(d-1)kU(\kappa/k)W^2(\kappa/k)}{2(2\pi)^d[W(\kappa/k)+\mu_R k^{z-2}]} \times \begin{cases} W(\kappa/k) \text{ for } z<2 \\ \mu_R k^{z-2} \text{ for } z>2 , \end{cases} \tag{3.35}$$

to the zero-loop order. By using the same argument, it is possible to obtain the velocity time correlation function

$$\langle \mathbf{v}(\mathbf{r},t)\mathbf{v}(\mathbf{r},0)\rangle = \frac{2\overleftrightarrow{1}}{d}\int_0^\infty dk\, E(k)\frac{\mu_R k^{z-2}e^{-W(\kappa/k)k^2|t|}-W(\kappa/k)e^{-\mu_R k^z|t|}}{\mu_R k^{z-2}-W(\kappa/k)} . \tag{3.36}$$

Before examining the possible choices of the exponents, two related points must be considered; namely, where does the dissipative range appear in our theory and have relevant variables been omitted from the theory. The latter is particularly important, since it is well known that omitting symmetry-allowed, relevant terms from the theory will result in divergences, even if they accidentally do not appear at low order in the loop expansion.

The noise model, cf. Eq. (2.1), cannot be valid at all scales. As was discussed in the Introduction, the noise itself is, at least in part, a consequence of projecting out the long-wavelength scales, L. As such, we do not expect that the theory will be able to say anything meaningful about these scales; i.e., about the scales where the details of the boundaries, etc., become important.

At sufficiently short wavelengths another scale becomes important; i.e., the dissipative scale l_d. In this range the viscous forces dominate and the turbulent motion should decay rapidly. At present, none of the applications of renormalization-group methods produces the expected behavior in the dissipative range. Indeed, as was mentioned in Sec. II, the noise model has an implied upper as well as lower, wave-vector cutoff. Moreover, the need for an upper cutoff becomes most clear for cases with negative y. What is the upper cutoff? The obvious choice is l_d^{-1}.

The renormalization-group method provides a prescription for resumming terms in the naive perturbation expansion which depend strongly on the implied cutoffs (both upper and lower) near the critical dimension. Thus, while the analysis considers the behavior of certain subseries in the perturbation expansions in the limit of an infinite upper cutoff, in reality a finite, albeit large, uv cutoff still exists. The physical phenomena which occur at or above the cutoff scales will result in additional terms being generated in the Lagrangian, i.e., in Eq. (2.3), and it is necessary to see to what extent these terms can change the results obtained so far.

For example, consider a term containing m powers of $\mathbf{v}$, n powers of $\bar{\mathbf{v}}$, and q gradients, where Galilean invariance and momentum conservation [31] imply that $q\geq m+n$ for $m>2$. In addition, causality implies that $n\geq 1$. Simple dimensional analysis shows that $c^q_{m,n}$, the coefficient of this term, has engineering dimension $D^q_{m,n}\equiv md_v+nd_{\bar{v}}-q+d+d_\Omega$, where $d_v\equiv 1-d_\Omega$, $d_{\bar{v}}\equiv d_\Omega-d-1$, and where we have assumed that $\omega\sim k^{d_\Omega}$. Moreover, since these terms arise from the behavior of the system in the dissipative range, we expect that $c^q_{m,n}=l_d^{-D^q_{m,n}}\hat{c}^q_{m,n}$, where $\hat{c}^q_{m,n}=O(1)$.

If the steps leading to the scaling form for an arbitrary quantity, cf. Eq. (3.29), are repeated with $c^q_{m,n}$ included, we find that

$$F=k^{-l}[W(\kappa/k)k^2]^{-\tau} \times G\left[\frac{\mu_R k^{z-2}}{W(\kappa/k)}, U(\kappa/k),\ldots,(kl_d)^{-D^q_{m,n}}\hat{c}^q_{m,n},\ldots\right] ,$$

where we have again ignored the possibility of field renormalization and have omitted the wave-vector and frequency arguments.

It is easy to show that $D^q_{m,n}<0$ for reasonable choices of q or d_Ω. This implies that the extra terms drop out of the calculation for $kl_d\to 0$, and hence they are irrelevant in the renormalization-group sense at the ir fixed point. This is analogous to the observation made in Ref. [14]. In addition, however, the preceding discussion shows

that they are unimportant for scales longer than those characterizing the dissipative range; i.e., for $kl_d \ll 1$. Nonetheless, even though the dissipation scale does not explicitly appear in the low-order results, it must be remembered that the omitted terms cannot be ignored in the dissipative range. We will return to this point when discussing our results.

We now turn to the analysis of the scaling properties of the theory and the choice of exponents which results in Kolmogorov's $\frac{5}{3}$ law. To this end, we need the asymptotic behaviors of $U(x)$ and $W(x)$, which follow from Eqs. (3.27) and (3.28):

$$U(x)=\begin{cases}\dfrac{u_R u^* x^{\varepsilon}}{(u^*-u_R)} & \text{as } x^{\varepsilon}\to 0\\ u^* & \text{as } x^{\varepsilon}\to\infty\end{cases} \tag{3.37}$$

and

$$W(x)=\begin{cases}\nu_R\left[\dfrac{u^*}{u^*-u_R}\right]^{-\sigma\gamma/\varepsilon} & \text{as } x^{\varepsilon}\to 0\\ \nu_R {u^*}^{-\sigma\gamma/\varepsilon} x^{\sigma\gamma} & \text{as } x^{\varepsilon}\to\infty\ .\end{cases} \tag{3.38}$$

In identifying the exponents, three criteria must be satisfied: (1) The dynamic exponent corresponding to the cascade region must equal $\frac{2}{3}$, which is deduced from the Obukhov-Kolmogorov law for viscosity; (2) the energy spectrum must satisfy the $\frac{5}{3}$ law; and (3) the total energy of the fluid must be extensive, and hence, the kinetic energy spectrum must be ir integrable.

At this point, we shall present the analysis of the different ranges of z separately.

A. $z \geq 2$

We first examine the behavior for $z > 2$. In this case, the Wilson functions, and hence, the functions U and W are identical to those obtained in Ref. [17]. Nonetheless, the energy spectrum and the time correlation are not exactly the same.

We have two different dynamic exponents, one corresponding to decay rate $W(\kappa/k)k^2$, the other corresponding to decay rate $\mu_R k^z$ [see, e.g., Eq. (3.36)]. Clearly, since $z > 2$, the latter does not provide Kolmogorov's dynamic exponent, and hence, only $W(\kappa/k)k^2$ may give the expected dynamical exponent for some choice of ε. For $\varepsilon > 0$ (or $\varepsilon < 0$), we have $W(\kappa/k)k^2 = \nu_R u^* \kappa^{\gamma} k^{2-\gamma}$ in the small- (or large-) k limit. This leads to the same conclusion as Ref. [17], namely, $\gamma = \frac{4}{3}$. Consequently, there are two scaling regions for the energy spectrum; i.e., for $\varepsilon < 0$

$$E(k)\propto\begin{cases}k^{z-\varepsilon-1} & \text{as } k\to 0\\ k^{-5/3} & \text{as } k\to\infty\ ,\end{cases} \tag{3.39}$$

or for $\varepsilon > 0$

$$E(k)\propto\begin{cases}k^{z-7/3} & \text{as } k\to 0\\ k^{1-\varepsilon} & \text{as } k\to\infty\ .\end{cases} \tag{3.40}$$

Note the $k\to 0$ limits of the preceding expressions are different than those obtained for white noise [17]; this is not surprising since the noise correlations decay very slowly in the ir limit when $z > 2$.

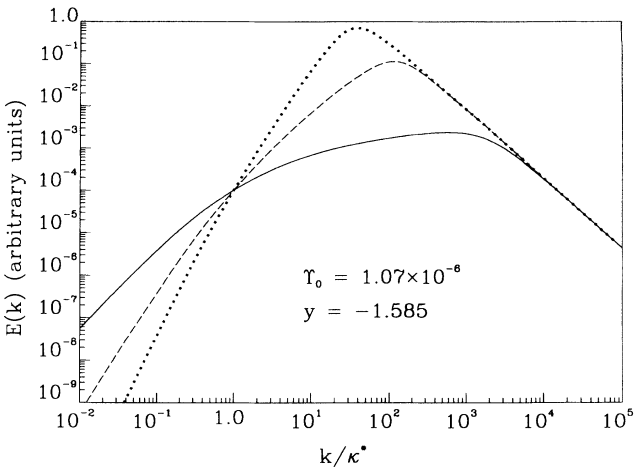

FIG. 3. Examples of the renormalized zero-loop kinetic energy spectrum for $z > 2$. The exponent y was chosen to give the $\frac{5}{3}$ law in the uv in three spatial dimensions (Ref. [17]), while Υ was set to the value obtained by fitting the experimental data in Ref. [34] (note, however, that the fit gives $z < 2$). The curves correspond to $z = 2.5$ (——), 3.5 (— — —), and 4.5 (· · · ·).

Since $z > 2$, the $\frac{5}{3}$ spectrum can be obtained only in the uv and only one choice can simultaneously give the correct exponent; i.e., that corresponding to $\varepsilon < 0$. This in turn leads to $y = -1.5851\ldots$, which is the same as was found in Ref. [17]. Note that the integrability and Galilean invariance criteria are automatically satisfied for this choice. Some examples of the kinetic energy spectrum are shown in Fig. 3.

The case $z = 2$ is special. It is easy to see from the definitions of the Wilson functions that the fixed-point values for U and W have the same values as when $z > 2$. Moreover, the linear-stability analysis of the characteristic equations gives the same stability exponents as when $z > 2$, and near the nontrivial fixed point $W(\kappa)\propto\kappa^{\gamma}$ while $U(\kappa)/u^* - 1 - 3\gamma W(\kappa)/[\mu_R(\gamma+\varepsilon)]\propto\kappa^{-\varepsilon}$.

In general, the characteristics may be computed from Eqs. (3.19), (3.20), (3.23), and (3.24), and some examples are shown in Figs. 4 and 5. Physically meaningful trajectories must be in the first quadrant of the W-U plane. Note the large swing that occurs when the trajectory starts at sufficiently large values of ν_R/μ_R.

B. $z < 2$

This case is more interesting, since the noise relaxation is slower than that of bare shear fluctuations in the uv limit. In principle, either $\omega_1(k)\equiv W(k)k^2 \sim k^{2-z_v}$ or $\omega_2(k)\equiv\mu_R k^z$ could be chosen to give the Obukhov-Kolmogorov $\frac{2}{3}$ law. In addition, the energy spectrum now has four scaling regions with exponents as shown in Table I. The four regions are ordered by increasing k, with regions I and IV corresponding to the ir and uv limits, respectively.

To proceed further, note that the renormalized equation of motion for the average flow is

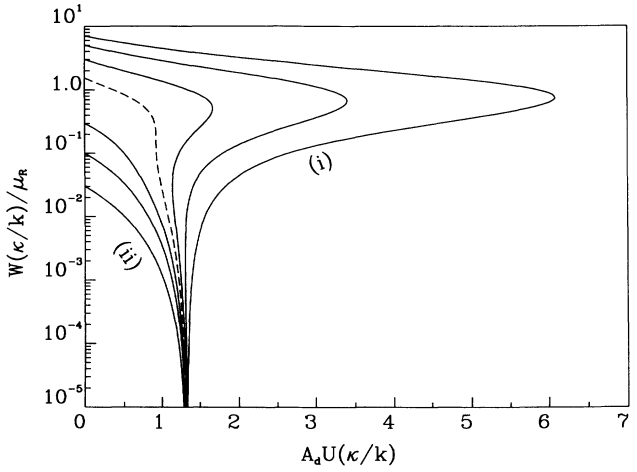

FIG. 4. The parameter flows when $z=2$, $d=3$ and $\gamma=\frac{4}{3}$ ($y=-1.585$). The last choice gives the usual Kolmogorov scaling; as was the case in Ref. [17], there are two choices of y which give this. The figure shows that corresponding to $\varepsilon<0$ (i.e., a nontrivial uv fixed point). The dashed curve separates the cases which can exhibit a swing.

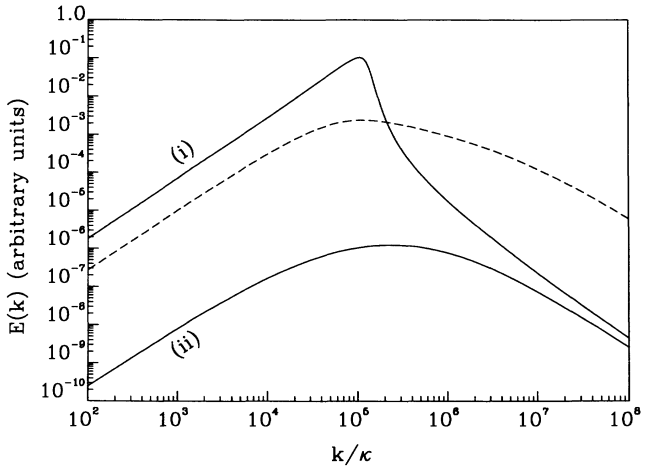

FIG. 5. Examples of the energy spectrum when $z=2$. The parameters are as in Fig. 4. The curve are labeled to correspond to the corresponding curves in Fig. 4.

$$[i\omega+W(\kappa/k)k^2]\langle v^\alpha(\mathbf{k},\omega)\rangle-\frac{iV_{\mathbf{k}}^{\alpha;\beta,\gamma}}{2(2\pi)^{d+1}}\int d\mathbf{k}_1 d\omega_1\langle v^\beta(\mathbf{k}-\mathbf{k}_1,\omega-\omega_1)\rangle\langle v^\gamma(\mathbf{k}_1,\omega_1)\rangle=0 \tag{3.41}$$

to zero-loop order. As was described above, the viscosity ν has been replaced by $W(\kappa/k)$. Hence, in order that the Obukhov-Kolmogorov $\frac{2}{3}$ law holds for the effective viscosity, we must chose $z_\nu=\sigma\gamma=\frac{4}{3}$. Furthermore, it is easy to see that the kinetic-energy spectrum is not ir integrable if $\varepsilon>0$. Hence, the only choices left require that $\varepsilon<0$.

It is straightforward to show that requiring $\sigma\gamma=\frac{4}{3}$ with $\varepsilon<0$ is possible if and only if $z>4-d$ (in addition, $z<2$, by assumption). Hence, when $d=3$, we require that $z>1$ and region III becomes the Kolmogorov region. This also meets the local Galilean invariance criterion for modeling the noise correlation.

Thus, for $u_R\neq u^*$, the energy spectrum may be rewritten as

$$E(k)=\frac{S_d(d-1)u^*\nu_R^2\kappa\tau^{5/3\varepsilon}q^{3-\varepsilon-z}}{2(2\pi)^d(q^{-\varepsilon}+1)^{1-4/\varepsilon}[q^{2-z}(q^{-\varepsilon}+1)^{4/3\varepsilon}+\Upsilon]}\ , \tag{3.42}$$

where $q\equiv k/\kappa^*$, $\kappa^*\equiv\kappa\tau^{-1/\varepsilon}$, $\tau\equiv(u^*-u_R)/u_R$, and $\Upsilon\equiv(1+\tau)^{4/3\varepsilon}\tau^{(2-3z)/3\varepsilon}\mu_R\kappa^{z-2}/\nu_R$.

Some examples of the energy spectrum are shown in Fig. 6. Figure 7 presents effective scaling exponents for the energy spectrum for different values of Υ. Plateaus indicate scaling regions of $E(k)$. Note that the scale characterizing the maximum of $E(k)$ is roughly κ^* and not the renormalization scale κ. This implies that the crossover between region II and region III, i.e., the lower end of the inertial range, can be modified by changing τ.

As Fig. 7 shows, whether all four scaling regions occur depends on the value of Υ. Since $1<z<2$ and $\varepsilon<0$, the maximum value of $q^{2-z}(q^{-\varepsilon}+1)^{4/3\varepsilon}$, i.e.,

$$\Upsilon_c\equiv\left[\frac{(2-z)^{2-z}(z-\frac{2}{3})^{z-2/3}}{(\frac{4}{3})^{4/3}}\right]^{-1/\varepsilon}\ , \tag{3.43}$$

is less than unity. Roughly speaking, therefore, regions I and IV disappear for $\Upsilon\ll\Upsilon_c$, while regions II and III vanish for $\Upsilon>\Upsilon_c$. Note that the small-k regions have

TABLE I. Scaling exponents for $z<2$.

	Exponents		Region I	Region II	Region III	Region IV
$\varepsilon<0$	$z>2-\sigma\gamma$	η	$\varepsilon+z-3$	$\varepsilon-1$	$2\sigma\gamma-1$	$3\sigma\gamma-3+z$
	$z=2-\sigma\gamma$		$\varepsilon+z-3$	$\varepsilon-1$	$2\sigma\gamma-1$	$2\sigma\gamma-1$
	$z<2-\sigma\gamma$		$\varepsilon+z-3$	$\varepsilon-1$	$3\sigma\gamma-3+z$	$2\sigma\gamma-1$
		z_ν	0	0	$\sigma\gamma$	$\sigma\gamma$
$\varepsilon>0$	$z>2-\sigma\gamma$	η	$2\sigma\gamma-1$	$3\sigma\gamma-3+z$	$\varepsilon+z-3$	$\varepsilon-1$
	$z=2-\sigma\gamma$		$2\sigma\gamma-1$	$2\sigma\gamma-1$	$\varepsilon+z-3$	$\varepsilon-1$
	$z<2-\sigma\gamma$		$3\sigma\gamma-3+z$	$2\sigma\gamma-1$	$\varepsilon+z-3$	$\varepsilon-1$
		z_ν	$\sigma\gamma$	$\sigma\gamma$	0	0

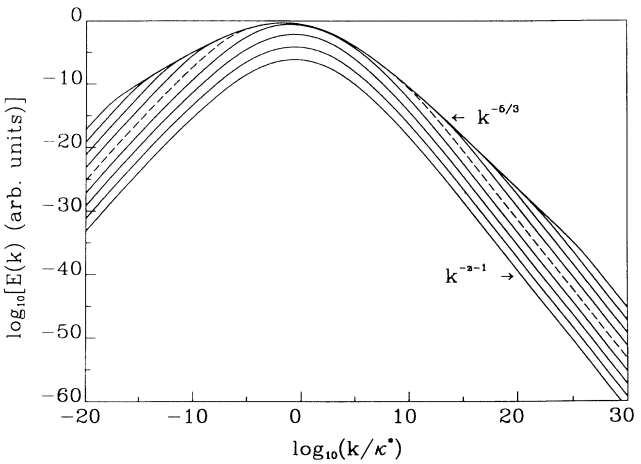

FIG. 6. Examples of the energy spectrum for $z<2$ in $d=3$. Curves correspond to $\sigma\gamma=\frac{4}{3}$, $z=1.21$, cf. Eq. (3.42), and Υ ranging from 1.07×10^{-11}, 1.90×10^{-10}, 3.38×10^{-9}, 6.02×10^{-8}, 1.07×10^{-6} (dashed, this value is obtained from the fitting of experiment data of Ref. [34]), 1.90×10^{-5}, 3.38×10^{-4}, 6.02×10^{-3}, and 1.07×10^{-1}.

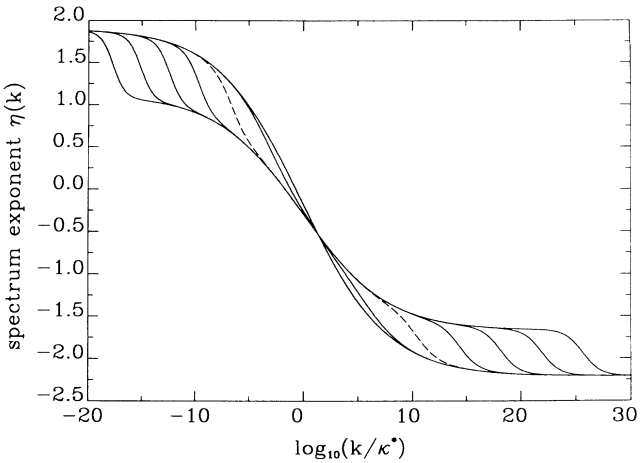

FIG. 7. The effective-energy spectrum scaling exponent, defined as $\eta(k)\equiv d\ln E(k)/d\ln k$ when $z<2$. The dashed curve corresponds to $\sigma\gamma=\frac{4}{3}$, $z=1.21$, and $\Upsilon=1.07\times10^{-6}$. These values were obtained by fitting the experimental results of Ref. [34]. The other curves correspond to the values of Υ used in Fig. 6.

positive exponents for the energy spectrum and describe the projections of the L-scale motion of the problem; hence, the form of the noise correlation and its exponents are probably not universal in regions I and II.

In the high-k regions, we observe a crossover between region III, the Kolmogorov region, and region IV, where the crossover wave vector depends on the value of Υ. We tentatively identify region IV as the intermittency region. In order to examine this possibility further, we now examine the role of the Reynolds number in determining Υ and the crossover wave vector.

We define the Reynolds number R_e by

$$R_e \equiv \frac{[\langle |\mathbf{v}(\mathbf{r},t)|^2\rangle]^{1/2}}{\kappa\nu_R} = \frac{\left[2\int_0^\infty dk\, E(k)\right]^{1/2}}{\kappa\nu_R} . \tag{3.44}$$

Note that Eq. (3.44) is sensible only if the proportionality constant relating ν and ν_R is independent of R_e. This will be the case when $u_R \to u^*$; i.e., as is the case for large enough R_e, cf. Eq. (3.46) below.

By using the zero-loop equation of motion, Eq. (3.41), it is easy to show that the renormalized effective rate of energy dissipation is

$$\langle\varepsilon\rangle = 2\int_0^\infty dk\, k^2 W(\kappa/k)E(k) . \tag{3.45}$$

This expression together with Eq. (3.44) may be used to reexpress Υ in terms $\langle\varepsilon\rangle$ and R_e. For example, when $u_R \to u^*$ it follows that

$$R_e \approx r_d^{1/2}\left[\frac{u^*-u_R}{u_R}\right]^{1/3\varepsilon} = r_d^{1/2}\tau^{1/3\varepsilon} , \tag{3.46}$$

where $r_d \equiv 4d(d^2+d-2)/[3(d^2-d+2)]$. Since $\varepsilon<0$, the fixed point $U=u_R=u^*$ corresponds to the large-Reynolds-number limit. In the same limit (i.e., $R_e\to\infty$), we also have

$$\kappa^* \approx \kappa\left[\frac{R_e}{\sqrt{r_d}}\right]^{-3} \tag{3.47}$$

and

$$\Upsilon \approx e^{-\langle\varepsilon\rangle(3z-2)/\varepsilon_0} . \tag{3.48}$$

where $\varepsilon_0 \equiv r_d\kappa^4\nu_R^3/3$.

As $R_e\to\infty$, the small-scale motions of the fluid demand an infinite amount of external energy, and the energy dissipation diverges. If we assume power-law behavior for the dissipation rate; i.e., $\langle\varepsilon\rangle/\varepsilon_0 \sim R_e^\alpha$ (in the Kolmogorov case, $\alpha=3$) it follows that Υ goes to zero monotonically as $R_e\to\infty$. Thus, Υ and κ^* vanish as the Reynolds number is increased, and the $k^{-5/3}$ energy spectrum is found at all scales. Conversely, the Kolmogorov cascade (region III) vanishes when $\Upsilon>\Upsilon_c$ and only the intermittency region (region IV) remains. This last limit can approached by reducing the Reynolds number, although whether a fully intermittent spectrum can be seen before the flow becomes laminar (and hence, the basic assumption about the form of the noise correlation breaks down) is unclear.

The Reynolds number dependence of the crossover scales l_c and dissipative scale l_d can now be examined. When Eqs. (3.47) and (3.48) are used in the zero-loop energy spectrum, cf. Eq. (3.42), it follows that

$$\kappa l_c \approx \left[\frac{R_e e^{-\langle\varepsilon\rangle/\varepsilon_0}}{\sqrt{r_d}}\right]^3 . \tag{3.49}$$

Hence, for large R_e, the crossover scale is a strongly decreasing function of the Reynolds number. On the other hand, the dissipative scale has a much weaker R_e dependence; i.e. [3],

$$l_d \sim L/R_e^{3/4} .$$

Since the theory is valid only for scales longer than the disspative scale, we conclude that the intermittency region will rapidly merge with the dissipative region, and hence disappear, as the Reynolds number is increased.

In the high-k scaling regions, i.e., when $k > \kappa^*$, the energy spectrum can be written as

$$E(k) = C_{\rm Kol}\varepsilon_0^{2/3}\frac{k^{-5/3}}{1+(kl_c)^{z-2/3}} , \tag{3.50}$$

where

$$C_{\rm Kol} = \frac{9\sigma\gamma}{8}\left[\frac{4d(d+2)(d-1)}{9(d^2-d+2)}\right]^{1/3} . \tag{3.51}$$

With the Kolmogorov choice $\sigma\gamma = \frac{4}{3}$, we find that $C_{\rm Kol} = 1.778$ when $d = 3$. The experimental value for this universal number is $1.3-2.3$ depending on methods of determining the constant [5]. Also note that the exponent in the Kolmogorov theory of intermittency [4] discussed in the introduction is given by $B = z - \frac{2}{3}$.

IV. SOME APPLICATIONS

We have seen that, the $z > 2$ case is very similar to what was found in Refs. [17] and [32] and will not be pursued further. On the other hand, a new crossover is found when $z < 2$ and its effect on other observable quantities is now examined.

A. Skewness

A complete description of the turbulent flow should produce the distribution function of the velocity fields, or equivalently, the moments or central moments of the velocity fields of *all* orders [5]. In practice, our calculation is limited to a few leading-order moments due to the difficulties in performing the integrals.

As has been mentioned in the Introduction, one of the important quantities which characterizes the velocity distribution is the skewness of the two-point probability distribution as defined in Eq. (1.1). For a homogeneous fluid it follows that

$$T(r) \equiv \langle [v_r(\mathbf{r},t) - v_r(0,t)]^3 \rangle = 6\langle v_r(\mathbf{r},t) v_r^2(0,t) \rangle , \tag{4.1}$$

and

$$b(r) \equiv \langle [v_r(\mathbf{r},t) - v_r(0,t)]^2 \rangle = 2[\langle v_r(0,t) v_r(0,t) \rangle - \langle v_r(\mathbf{r},t) v_r(0,t) \rangle] , \tag{4.2}$$

provided that $\langle v_r(\mathbf{r},t) \rangle = 0$. Hence,

$$s(r) = \frac{T(r)}{b(r)^{3/2}} , \tag{4.3}$$

cf. Eq. (1.1). For turbulent fluid exhibiting Kolmogorov scaling, it is easy to show [3,4,5,33] that $T(r) \propto r$ and $b(r) \propto r^{2/3}$. Thus $s(r) = \text{const}$. For an intermittent fluid, it has been proposed [4] that $s(r)$ diverges as $r \to 0$.

Our theory predicts an extra scaling region (region IV) beyond the Kolmogorov region (region III). From the energy spectrum, we tentatively associated this extra region with intermittency, since it falls off more rapidly than in the Kolmogorov cascade. In order to see if the velocity distribution is nontrivial, it is important to examine the small-r behavior of some of the additional moments, e.g., the skewness.

To the zero-loop order, the second-order moment is

$$b(r) = \frac{8S_{d-1}}{(d-1)S_d}\int_0^\infty dk\, E(k) Z_1^{(d)}(kr) , \tag{4.4}$$

where

$$Z_1^{(d)}(x) \equiv \frac{\sqrt{\pi}}{2}\frac{\Gamma\left[\frac{d+1}{2}\right]}{\Gamma\left[\frac{d+2}{2}\right]} \times \left[1 - \frac{d}{2}\left[\frac{2}{x}\right]^{d/2}\Gamma\left[\frac{d}{2}\right]J_{d/2}(x)\right] \tag{4.5a}$$

and $J_\nu(x)$ is a Bessel function of the first kind. When $d = 3$,

$$Z_1^{(3)}(x) = 2\left[\frac{1}{3} - \frac{\sin(x)}{x^3} + \frac{\cos(x)}{x^2}\right] . \tag{4.5b}$$

By using Eq. (3.50), it follows that the crossover between region III and region IV occurs around $k_c \equiv l_c^{-1}$. In addition, Eq. (3.42) or Table I show that

$$E(k) \propto \begin{cases} k^{-5/3} \text{ for } k_c > k > \kappa^* \\ k^{-1-z} \text{ for } k > k_c , \end{cases} \tag{4.6}$$

and thus

$$b(r) \propto \begin{cases} r^{2/3} \text{ for } l_c < r < l^* \\ r^z \text{ for } r < l_c , \end{cases} \tag{4.7}$$

where $l^*\kappa^* \equiv 1$.

The third-order moment to the zero-loop order is

$$T(r) = \frac{48S_{d-1}}{(2\pi)^d}\int_0^\infty dk\, C(k) Z_2^{(d)}(kr) , \tag{4.8}$$

where

$$Z_2^{(d)}(x) \equiv \frac{\sqrt{\pi}}{4}\left[\frac{2}{x}\right]^{d/2}\Gamma\left[\frac{d+1}{2}\right]J_{1+d/2}(x) . \tag{4.9}$$

When $d = 3$,

$$Z_2^{(3)}(x) = \frac{1}{x^4}[(3-x^2)\sin(x) - 3x\cos(x)] . \tag{4.9a}$$

In addition,

$$C(k) \equiv \frac{2k^{d-1}}{(d-1)(2\pi)^d}\int d\mathbf{k}_1 \{t_a[f(k,k_1,k_p) - f(k_p,k,k_1)] + t_b[f(k_1,k_p,k) - f(k_p,k,k_1)]\} , \tag{4.10}$$

where

$$t_a \equiv \frac{kk_1[xk+(d-2+2x^2)k_1](1-x^2)}{k_p^2} , \tag{4.10a}$$

$$t_b \equiv -\frac{[xk_1+(d-2+2x^2)k](1-x^2)}{k_p^2} , \tag{4.10b}$$

$$k_p \equiv |\mathbf{k}+\mathbf{k}_1| , \tag{4.10c}$$

$$x \equiv \hat{\mathbf{k}}\cdot\hat{\mathbf{k}}_1 , \tag{4.10d}$$

and

$$\begin{aligned} f(k_1,k_2,k_3) \equiv & \left[\frac{(2\pi)^d}{S_d}\right]^2 \frac{U(\kappa/k_2)U(\kappa/k_3)[W(\kappa/k_2)k_2^2 W(\kappa/k_3)k_3^2]^3(k_2k_3)^{-2-d}}{[W(\kappa/k_2)k_2^2+\mu_R k_2^z][W(\kappa/k_3)k_3^2+\mu_R k_3^z]} \\ & \times \frac{1}{[W(\kappa/k_1)k_1^2+W(\kappa/k_2)k_2^2+\mu_R k_3^z][W(\kappa/k_1)k_1^2+\mu_R k_2^z+W(\kappa/k_3)k_3^2]} \\ & \times \frac{1}{[W(\kappa/k_1)k_1^2+\mu_R k_2^z+\mu_R k_3^z][W(\kappa/k_1)k_1^2+W(\kappa/k_2)k_2^2+W(\kappa/k_3)k_3^2]} \\ & \times \{W(\kappa/k_2)k_2^2\mu_R k_2^z[W(\kappa/k_1)k_1^2+\mu_R k_2^z+W(\kappa/k_2)k_2^2] \\ & + W(\kappa/k_3)k_3^2\mu_R k_3^z[W(\kappa/k_1)k_1^2+\mu_R k_3^z+W(\kappa/k_3)k_3^2] \\ & + [W(\kappa/k_1)k_1^2+\mu_R k_2^z+W(\kappa/k_2)k_2^2][W(\kappa/k_1)k_1^2+\mu_R k_3^z+W(\kappa/k_3)k_3^2] \\ & \times [W(\kappa/k_1)k_1^2+\mu_R k_2^z+W(\kappa/k_2)k_2^2+\mu_R k_3^z+W(\kappa/k_3)k_3^2]\} . \end{aligned} \tag{4.11}$$

After some straightforward, but lengthy algebra, the asymptotic behavior of $C(k)$ is obtained in the various scaling regions; thus,

$$C(k) \propto \begin{cases} k^{4-z-\varepsilon} \text{ for } k<\kappa^*\Upsilon^{1/(2-z)} \\ k^{2-\varepsilon} \text{ for } \kappa^*\Upsilon^{1/(2-z)}<k<\kappa^* \\ k^{-2} \text{ for } \kappa^*<k<k_c \\ k^{-z-8/3} \text{ for } k_c<k . \end{cases} \tag{4.12}$$

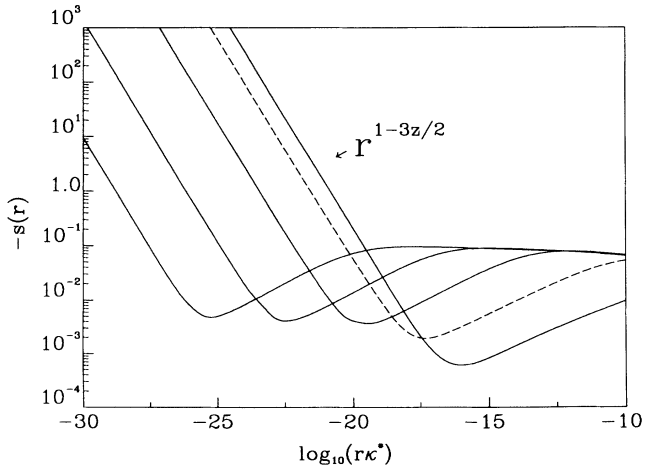

FIG. 8. Normalized skewness of the radial velocity distribution function. The curves correspond to $z=1.21$ and $\Upsilon=1.07\times10^{-11}$, 4.97×10^{-10}, 2.31×10^{-8}, 1.07×10^{-6} (dashed), and 4.97×10^{-5}, reading from left to right, respectively. As in Fig. 7, the dashed curve corresponds to the experiment in Ref. [34].

A naive scaling argument would suggest that $T(r)\propto r^{z+5/3}$ as $r\to0$. However, a more careful analysis shows that $T(r)\propto r$ for $r\ll l_c$, and hence,

$$s(r) \propto \begin{cases} \text{const for } l_c<r<l^* \\ r^{1-3z/2} \text{ for } r\ll l_c . \end{cases} \tag{4.13}$$

The integrals in Eqs. (4.10), (4.8), and (4.4) were performed numerically and the results are shown in Fig. 8. Note the divergence of $s(r)$ at small enough r.

The behavior of the skewness at $r\ll l_c$ supports our interpretation that region IV of the energy spectrum is indeed a nontrivial region describing intermittency. The energy spectrum decays faster than predicted by the Kolmogorov argument and there are strong deviations from Gaussian statistics. We recover the Kolmogorov picture for a fixed value of $r\kappa^*$ in the large-Reynolds-number limit. Note that if r is kept in region IV, it follows that

$$s(r) \propto \Upsilon^{3/2}\kappa^{*\,1-3z/2} r^{1-3z/2} , \tag{4.14}$$

and since Υ tends to zero exponentially, the coefficient will go to zero as the Reynolds number diverges. Of course, the comments concerning region IV and dissipative scale still apply.

B. Diffusion of a passive scalar

A passive scalar field such as temperature, concentration, etc. will be denoted as $S(\mathbf{r},t)$ and satisfies the following equation:

$$(i\omega+Dk^2)S(\mathbf{k},\omega)-\frac{i\bar{\lambda}}{(2\pi)^{d+1}}\int d\mathbf{k}_1 d\omega_1 \mathbf{k}\cdot\mathbf{v}(\mathbf{k}-\mathbf{k}_1,\omega-\omega_1)S(\mathbf{k}_1,\omega_1)=0 \ . \tag{4.15}$$

Thermal noise is ignored, D is the diffusivity, and $\bar{\lambda}$ plays the same role as λ in Eq. (2.3).

The passive scalar introduces two new terms in the Lagrangian; namely,

$$\mathcal{L}_0\equiv\frac{1}{(2\pi)^{d+1}}\int d\mathbf{k}\, d\omega i(i\omega+Dk^2)\tilde{S}(-\mathbf{k},-\omega)S(\mathbf{k},\omega) \tag{4.16}$$

and

$$\mathcal{L}_1\equiv\frac{\bar{\lambda}}{(2\pi)^{2(d+1)}}\int d\mathbf{k}d\omega d\mathbf{k}_1 d\omega_1 \tilde{S}(-\mathbf{k},-\omega)\mathbf{k}\cdot\mathbf{v}(\mathbf{k}-\mathbf{k}_1,\omega-\omega_1)S(\mathbf{k}_1,\omega_1) \ , \tag{4.17}$$

where $\tilde{S}(\mathbf{k},\omega)$ is the adjoint field to $S(\mathbf{k},\omega)$. We shall include $\mathcal{L}_0$ with the other quadratic terms in the analysis. Since there is no coupling between $\mathbf{v}$ and S in the free theory, it is easy to show that

$$\langle\tilde{S}(\mathbf{k},\omega)S(\mathbf{k}',\omega')\rangle_0=\frac{i(2\pi)^{d+1}\delta(\mathbf{k}+\mathbf{k}')\delta(\omega+\omega')}{-i\omega+Dk^2}\equiv$$ 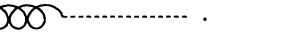 . (4.18)

The only primitively divergent diagram which appears at one-loop order is shown in Fig. 9, and power counting arguments show that it is marginal when $\varepsilon=0$. In addition, there is no divergent correction to $\bar{\lambda}$, and as was the case with λ in Sec. II, we henceforth let $\bar{\lambda}=1$. The renormalized diffusivity may be written in a form analogous to Eqs. (3.1)–(3.6), i.e.,

$$iD+\bar{\lambda}^2K_D=iD_R \ , \tag{4.19}$$

where

$$K_D=\frac{2i\chi\mu^2}{(2\pi)^{d+1}}\int d\mathbf{k}_1 d\omega_1\frac{\hat{\mathbf{k}}\cdot\overleftrightarrow{\Phi}_{\mathbf{k}_1}\cdot\hat{\mathbf{k}}k_1^{-y+2z}}{(\omega_1^2+\mu^2k_1^{2z})(\omega_1^2+\nu^2k_1^4)[-i(\omega-\omega_1)+D|\mathbf{k}-\mathbf{k}_1|^2]} \tag{4.20}$$

to one-loop order. For $z<2$, we find that the singular part of the right-hand side of Eq. (4.20) is

$$K_D\approx\frac{i\chi\mu\bar{\sigma}A_d}{\nu^2D\varepsilon} \ , \tag{4.21}$$

where

$$\bar{\sigma}\equiv\frac{2(d+2)(d-1)}{d^2-2} \ . \tag{4.22}$$

The relationship between the bare and renormalized diffusivities is obtained when the last result is used in Eq. (4.19); thus

$$D=D_R\left[1-\frac{\bar{\sigma}A_d u_R\nu_R^2}{D_R^2\varepsilon}\right] \ , \tag{4.23}$$

and the corresponding Wilson function becomes

$$\beta_D\equiv\kappa\left[\frac{\partial D_R}{\partial\kappa}\right]_{\nu,\chi,D}=-\frac{\bar{\sigma}A_d u_R\nu_R^2}{D_R} \ . \tag{4.24}$$

Finally, by defining the Prandtl number as $P\equiv\nu/D$, we obtain the characteristic equation for a scale-dependent renormalized Prandtl number; i.e.,

$$\kappa\frac{dP}{d\kappa}=\bar{\sigma}A_d UP(P^{*2}-P^2) \ , \tag{4.25}$$

with the initial condition $P(\kappa=1)=P_R\equiv\nu_R/D_R$. The fixed-point value is $P^*\equiv[(d^2-d+2)/(d^2+d-2)]^{1/2}$ is a universal number. When $d=3$, $P^*=\sqrt{0.8}\approx0.894$ (experimental values of P^* range from 0.7 to 0.9).

In general, the solution to Eq. (4.25) is

$$P(\kappa/k)=P^*\left\{1+\left[\frac{P^{*2}}{P_R^2}-1\right]\left[\frac{u^*}{u_R(k/\kappa)^{-\varepsilon}+u^*-u_R}\right]^{2\sigma\gamma/\varepsilon}\right\}^{-1/2} \tag{4.26a}$$

$$=P^*\left\{1+\left[\frac{P^{*2}}{P_R^2}-1\right]\left[\frac{R_e}{\sqrt{r_d}}\right]^{-6\sigma\gamma}\left[\frac{1+(R_e/\sqrt{r_d})^{3\varepsilon}}{(k/\kappa^*)^{-\varepsilon}+1}\right]^{2\sigma\gamma/\varepsilon}\right\}^{-1/2} \ , \tag{4.26b}$$

FIG. 9. Primitively divergent one-loop correction to the passive scalar diffusion constant.

where we have used the same match condition as was discussed in Sec. II as well as the solution to Eq. (3.23), i.e., Eq. (3.27). The second equality follows when Eqs. (3.46) and (3.47) are used to introduce the Reynolds number. In addition, in order that the diffusivity always be real, it is necessary that $P_R \leq P^*$. As Eq. (4.26b) shows, a universal Prandtl number should be observed when

$$\left[\frac{k}{\kappa}\right]^{-\varepsilon}+\left[\frac{R_e}{\sqrt{r_d}}\right]^{3\varepsilon}\lesssim\left[\frac{P^{*2}}{P_R^2}-1\right]^{\varepsilon/(2\sigma\gamma)}.$$

Hence, even at infinite R_e a universal Prandtl number is observed only in part of the inertial range, namely, for $k\lesssim\kappa(P^{*2}/P_R^2-1)^{-2/\sigma\gamma}$. This defines the top of the convective-inertial range [5]. For larger wave vectors, $P(k)\sim k^{-\sigma\gamma}\to 0$, which reflects the effective diffusivity becoming constant at smaller scales.

The nontrivial fixed point is stable in the ir and in the large-Reynolds-number limit. In the low-wave-vector end of the convective-inertial range (i.e, for $k\sim\kappa^*$), using the choice of $\sigma\gamma$ which gives the Kolmogorov $\frac{5}{3}$ law, we find that

$$P(\kappa/k)-P^*\sim-\frac{P^*}{2}\left[\frac{P^{*2}}{P_R^2}-1\right]\left[\frac{R_e}{\sqrt{r_d}}\right]^{-8}, \tag{4.27}$$

and hence, the Reynolds-number correction exponent is universal.

Finally, note that if an additive noise source is included in Eq. (4.15), it is easy to construct the source correlation (either for white or colored noise) such that additional primitive divergences, with concomitant renormalization conditions, are obtained. Nonetheless, it is easy to see that these will not change any of the results for the effective diffusion constant obtained with the noise omitted. (This is obviously not the case for the spectrum of the passive scalar fluctuations.)

C. Homodyne-scattering spectrum

As was shown in Ref. [32], the homodyne-scattering experiments from turbulent flows performed by Tong, Goldburg and co-workers [10,34] can be analyzed in terms of the normalized homodyne-scattering function,

$$F(q,t)=\frac{2}{L^2}\int_0^L dr\,(L-r)\times e^{-\Phi_1(r,t)-[1-d\sin^2(\theta/2)]\Phi_2(r,t)}, \tag{4.28}$$

where L is the length of the detection region, $q=(4\pi/\lambda)\sin(\theta/2)$ is the momentum transfer, θ is the scattering angle, and λ the wavelength of the incident light. For short enough times [32], Φ_1 and Φ_2 become

$$\Phi_1(r,t)=\frac{2q^2t^2}{d}\int_0^\infty dk\,E(k)\left[1-\Gamma\left[\frac{d}{2}\right]\left[\frac{2}{kr}\right]^{(d-2)/2}\times J_{d/2-1}(kr)\right], \tag{4.29a}$$

and

$$\Phi_2(r,t)=\frac{2q^2t^2\Gamma\left[\frac{d}{2}\right]}{d(d-1)}\times\int_0^\infty dk\,E(k)\left[\frac{2}{kr}\right]^{(d-2)/2}J_{d/2+1}(kr). \tag{4.29b}$$

It is easy to show that $F(q,t)$ decays monotonically as time increases. Moreover, the major contributions to the integral in Eq. (4.28) comes from the region where $kr\gtrsim\pi$. Therefore, if

$$L^*\equiv L\kappa^*<1, \tag{4.30}$$

cf. Eq. (3.42), we expect the homodyne-scattering function to be dominated by the behavior of the energy spectrum in the inertial range. Hence, by using Eq. (3.42) for the energy spectrum, and letting $d=3$, we find that

$$F(q,t)=2\int_0^1 dy\,(1-y)\exp\left[-\frac{5(q\nu_R\kappa t)^2R_e^2(yL^*)^z}{3\Upsilon\sqrt{r_d}}\int_0^\infty dx\,\frac{x^{-5/3}g_\theta(x)}{x^{z-2/3}+(yL^*)^{z-2/3}/\Upsilon}\right], \tag{4.31}$$

where we have used Eq. (3.46) and where

$$g_\theta(x)\equiv 1-\frac{\sin(x)}{x}+\frac{2}{x^3}[1-3\sin^2(\theta/2)][(3-x^2)\sin(x)-3x\cos(x)]. \tag{4.32}$$

Since $\Upsilon\to 0$ when $R_e\to\infty$, it follows that

$$F(q,t)\approx 3[x^{-3}\gamma(\tfrac{3}{2},x^2)-x^{-6}\gamma(3,x^2)], \tag{4.33}$$

where, $\gamma(a,b)$ is an incomplete gamma function, and

$$x\equiv\left[\frac{3\Gamma(\frac{1}{3})}{4}\left[1+\frac{1-3\sin^2(\theta/2)}{11}\right]\right]^{1/2}(\kappa L)^{1/3}q\nu_R\kappa t. \tag{4.34}$$

As was shown in Ref. [28], Eq. (4.33) leads to a t^{-3} tail in $F(q,t)$. On the other hand, when region IV (i.e., intermittency) dominates, i.e., $L^* \to 0$ while keeping Υ finite, we find that

$$F(q,t) \approx \frac{2}{z}[x^{-2/z}\gamma(1/z,x^2) - x^{-4/z}\gamma(2/z,x^2)] , \tag{4.35}$$

where

$$x \equiv \left[\left[\frac{u_R}{u^*} \right]^{4/3\varepsilon} \frac{5\pi}{6\Gamma(2+z)\sin(\pi z/2)} \left[1 + \frac{z}{2(z+3)}[1-3\sin^2(\theta/2)] \right] \right]^{1/2} \Upsilon^{-1/2} \left[\frac{R_e}{\sqrt{r_d}} \right]^{1-3z/2} (\kappa L)^{z/2} q \nu_R \kappa t \ . \tag{4.36}$$

Now the homodyne-scattering function decays as $t^{-2/z}$, which is slower than the Kolmogorov case (recall that $1 < z < 2$).

As long as the Reynolds number is not too large, the exponent characterizing the tail of the homodyne-scattering function is a direct measure of z, cf. Eq. (4.35). The recent experiments of Tong *et al.* [34] measured the homodyne scattering function for small polystyrene spheres in turbulent flows with and without added polymer. When we extract the exponent z directly from the tail of the homodyne-scattering functions, we find that $z = 1.19 \pm 0.05$, for all the experimental scattering geometries used. A full nonlinear least-squares fit of $\ln[F(q,t)]$, cf. Eq. (4.28), to the polymer-free data given in Ref. [34] gives $z = 1.21 \pm 0.04$. An example is shown in Fig. 10.

Our analysis shows that the characteristic time for the decay of the homodyne function will scale like $(qL^{\zeta})^{-1}$, where the exponent ζ will take on different values depending on which scaling region dominates the homodyne-scattering function. In particular, when region III dominates (e.g., in the limit of infinite Reynolds number) $\zeta = \frac{1}{3}$, while in the intermittency region (IV) $\zeta = z/2$. Thus the Kolmogorov prediction should be approached from above as $R_e \to \infty$. This behavior was seen qualitatively in the experiments of Ref. [10] (although, there probably is a high degree of uncertainty in the exponents).

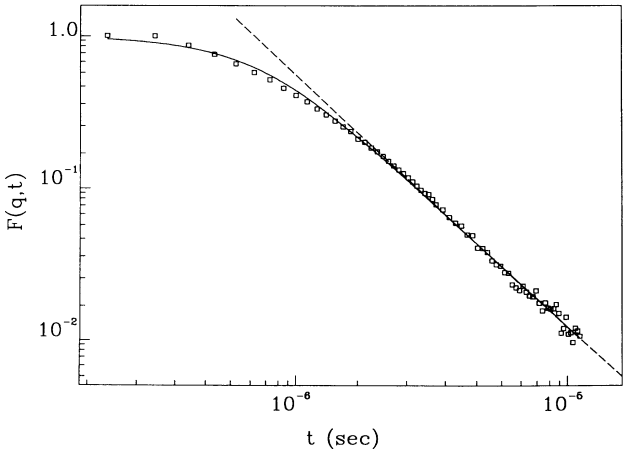

FIG. 10. Comparison of the theory to the experimental data of Ref. [34]. The dashed line indicates the direct fitting of the tail.

V. DISCUSSION

In this work, we have extended the renormalization-group analysis of the fluctuating Navier-Stokes equations to the case where the noise is colored both in time and space. As was the case with the earlier works in this area, it is possible to adjust the exponents characterizing the noise such that the Kolmogorov $\frac{5}{3}$ law is obtained in part of the kinetic-energy spectrum.

Like Ref. [17] and unlike Ref. [16], we can obtain Kolmogorov scaling behavior in something other than the $k \to 0$ limit, thereby obtaining an ir-integrable spectrum. It must be stressed that on this last point we differ from the work of Ref. [16]. Here both y and ε are negative, and $|\varepsilon| \ll 1$ (e.g., for the fits to the data of Ref. [34], $\varepsilon = -0.11$); the reverse is true in Ref. [16]. Since $y < 0$, the noise vanishes at long wave vectors, and in this sense our calculation is similar to model A of Forster, Nelson, and Stephen [14], as is our discussion of the qualitative behavior near the fixed points, relevant variables, etc. Nonetheless, including the noise renormalization, and carrying out the double expansion in ε and ε' allows us to construct an inertial range in part of the energy spectrum other than at $k = 0$.

As we have shown, when the correlation time of the noise is shorter than that corresponding to the bare viscous relaxation time, results equivalent to those obtained with a white-noise source are found. On the other hand, if the correlation time of the noise becomes longer than the bare viscous relaxation time, we find that the energy spectrum decays more quickly than in the inertial range. Moreover, while a scaling law is still obtained (i.e., in region IV), it is impossible to adjust the exponent to give the $\frac{5}{3}$ law if $d < 3\frac{1}{3}$ or for any d if the approximate Galilean invariance discussed in the Introduction is imposed. Finally, the skewness of the velocity distribution function shows marked deviations from the scaling predictions for nonintermittent flows. Based on these results, we have associated this new scaling regime with intermittency.

There is a crossover between the new scaling regime and that where the Kolmogorov $\frac{5}{3}$ law can be obtained. The crossover wave vector rapidly increases as the Reynolds number is increased, leaving behind the Kolmogorov energy spectrum at all scales where the theory is expected to be valid.

We have also examined the diffusion of a passive scalar. Here we find a universal Prandtl number in the lower part of the inertial range. Our value ($\sqrt{0.8}$) differs from

that obtained by Yakhot and Orszag [16] (0.7179), and this difference can be traced to the inclusion of the noise renormalization. In addition, we find that the convective-inertial range does not extend through the entire inertial range, and normal diffusion is found at smaller length scales, even in the limit of infinite Reynolds number.

There remain at least two main points for future consideration. The first concerns the applicability of the additive-noise model to turbulence. The problem we have considered is well posed and interesting in its own right, and gives results that seem to be applicable to turbulent flows. Nonetheless, a complete theory of turbulence should be able to demonstrate that the projected random force defined by Eq. (1.9) does indeed have some of the stochastic properties assumed in this work. Although it is easy to imagine applying a Wilson-Kadanoff decimation scheme to the longer scales, an analytic approach will require a model that can be approximately solved in closed form.

The second remaining point concerns the treatment of the dissipative range. As was discussed in Sec. III, renormalization-group methods will develop problems associated with relevant variables for sufficiently high wave vectors, and hence, there are restrictions on the wave vectors which can be considered. This is especially important in models which have random force spectra which *grow* with increasing wave vectors or do not give the $\frac{5}{3}$ law as the $k \to 0$ limit, e.g., as was the case here. Indeed, if the problem of determining the random force in an *a priori* fashion can be solved, it is likely that the resulting random-force spectrum will have a strong cutoff in the dissipative range, no matter what it looks like at smaller scales. How this cutoff, or other relevant quantities, can be incorporated into our results, thereby obtaining expressions which uniformly extrapolate into the dissipative regime, is at present an open question. Moreover, from our discussion of relevant and irrelevant variables, it is not clear that renormalization-group methods will be useful in the dissipative range.

In the future, we will present results for the spectrum of velocity fluctuations in the presence of nonzero average velocity gradients.

ACKNOWLEDGMENTS

Portions of this work were supported by the National Sciences and Engineering Research Council of Canada and by Le Fonds pour la Formation de Chercheurs et l'Aide à la Recherche du Québec. We also thank P. Tong for useful discussions.

[1] L. F. Richardson, *Weather Prediction by Numerical Process* (Cambridge University Press, Cambridge, 1922).
[2] A. N. Kolmogorov, C. R. Acad. Sci. USSR **30**, 301 (1941); **30**, 538 (1941).
[3] L. D. Landau and E. M. Lifshitz, *Fluid Mechanics, Landau and Lifshitz Course of Theoretical Physics*, 2nd ed. (Pergamon, New York, 1982), Vol. 6.
[4] A. N. Kolmogorov, J. Fluid Mech. **13**, 82 (1962).
[5] A. S. Monin and A. M. Yaglom, *Statistical Fluid Mechanics: Mechanics of Turbulence*, edited by J. L. Lumley (MIT Press, Cambridge, MA, 1975).
[6] U. Frisch, P. L. Sulem, and M. Nelkin, J. Fluid Mech. **87**, 719 (1978).
[7] B. Mandelbrot, J. Fluid Mech. **62**, 331 (1974); in *Turbulence and Navier-Stokes Equations*, edited by R. Temam, Lecture Notes in Mathematics Vol. 565 (Springer, Berlin, 1976).
[8] R. Benzi, G. Paladin, G. Parisi, and A. Vulpiani, J. Phys. A **17**, 3521 (1984).
[9] R. H. Kraichnan, Phys. Rev. Lett. **65**, 575 (1990).
[10] P. Tong, W. I. Goldburg, C. K. Chan, and A. Sirivat, Phys. Rev. A **37**, 2125 (1988); P. Tong and W. I. Goldburg, Phys. Fluids **31**, 2841 (1988); **31**, 3253 (1988).
[11] P. C. Martin, E. D. Siggia, and H. A. Rose, Phys. Rev. A **8**, 423 (1973).
[12] S. K. Ma and G. F. Mazenko, Phys. Rev. B **11**, 4077 (1975).
[13] P. C. Hohenberg and B. I. Halperin, Rev. Mod. Phys. **49**, 435 (1977); H. K. Janssen, in *Dynamical Critical Phenomena and Related Topics*, edited by C. P. Enz, Lecture Notes in Physics Vol. 104 (Springer-Verlag, Berlin, 1979), and references therein.
[14] D. Forster, D. R. Nelson, and M. J. Stephen, Phys. Rev. A **16**, 732 (1977).
[15] C. De Dominicis and P. C. Martin, Phys. Rev. A **19**, 419 (1979); J. D. Fournier and U. Frisch, *ibid.* **17**, 747 (1978); **28**, 1000 (1983).
[16] V. Yakhot and S. A. Orszag, Phys. Rev. Lett. **57**, 1722 (1986); J. Sci. Comput. **1**, 3 (1986); W. P. Dannevik, V. Yakhot, and S. A. Orszag, Phys. Fluids **30**, 1 (1987).
[17] D. Ronis, Phys. Rev. A **36**, 3322 (1987).
[18] See, e.g., S. R. de Groot and P. Mazur, *Non-Equilibrium Thermodynamics* (North-Holland, Amsterdam, 1962).
[19] See, e.g., D. Ronis, I. Procaccia, and J. Machta, Phys. Rev. A **22**, 714 (1980).
[20] E. M. Lifshitz and L. P. Pitaevskii, *Statistical Physics, Part 2, Landau and Lifshitz Course of Theoretical Physics*, 2nd ed. (Pergamon, New York, 1980), Vol. 9.
[21] R. F. Fox and J. E. Keizer, Phys. Rev. Lett. **64**, 249 (1990).
[22] The longitudinal parts of the Navier-Stokes equations and $\mathbf{f}(\mathbf{r},t)$ are trivially eliminated by using the incompressibility condition.
[23] For a typical noise-correlation function $\Omega(k,\omega)$, power-counting arguments show that corrections to Gaussian statistics are irrelevant (in the renormalization-group sense) in the scaling regions of the theory (as will be shown later) with the choice of $\varepsilon < 0$.
[24] See, e.g., M. Van Dyke, *An Album of Fluid Motion* (Parabolic, Stanford, 1982).
[25] B. S. De Witt, Phys. Rev. **162**, 1195 (1967); S. Coleman and E. Weinberg, Phys. Rev. D **7**, 1888 (1973), and references therein.
[26] See, e.g., D. J. Amit, *Field Theory, the Renormalization Group, and Critical Phenomena*, 2nd ed. (World Scientific, Singapore, 1984).
[27] G. 't Hooft and M. Veltman, Nucl. Phys. B **44**, 189 (1972); G. 't Hooft, *ibid.* **44**, 444 (1973).
[28] It is easy to see that the frequency-correction terms do not

diverge in the one-loop terms.

[29] See, e.g., P. Garabedian, *Partial Differential Equations* (Wiley, New York, 1964), Chap. 2.

[30] M. E. Fisher, in *Critical Phenomena*, edited by F. J. Hahne, Lecture Notes in Physics Vol. 186 (Springer-Verlag, Berlin, 1983); J. Rudnick, and D. R. Nelson, Phys. Rev. B **13**, 2208 (1976); Y. Drossinos, and D. Ronis, *ibid.*, **39**, 12 078 (1989).

[31] By this we mean that the random force in Eq. (1.8) is the divergence of a random stress.

[32] D. Ronis, Phys. Rev. A **38**, 874 (1988).

[33] A. N. Kolmogorov, C. R. Acad. Sci. U.S.S.R. **32**, 16 (1941).

[34] P. Tong, W. I. Goldburg, J. S. Huang, and T. A. Witten, Phys. Rev. Lett. **65**, 2780 (1990).